Appendix C

Supplementary Information for Chapter 4

C.1 Materials and Methods

C.1.1 General Considerations

All manipulations were carried out using standard Schlenk or glovebox techniques under an N_2 atmosphere. Solvents were deoxygenated and dried by thoroughly sparging with N_2, followed by passage through an activated alumina column in a solvent purification system by SG Water, USA LLC. Nonhalogenated solvents were tested with sodium benzophenone ketyl in tetrahydrofuran (THF) to confirm the absence of oxygen and water. Deuterated solvents were purchased from Cambridge Isotope Laboratories, Inc., degassed, and dried over activated 3-Å molecular sieves prior to use.

C.1.2 Reagents

HEH_2,[1] $PNPMoBr_3$,[2] [ColH]OTf,[2] $[P_3^BFe]BAr^F_4$ (P_3^B = tris[2-(diisopropylphosphino)phenyl]borane),[3] BTH_2,[4] $NaBAr^F_4$,[5] ^{15}N-Col,[6] $phenH_2$,[7] $phenazH_2$,[8] $[TBA][^{15}NO_3]$[9] were prepared according to literature procedures. Triflic acid, ethyl acetoacetate, and 37% aqueous formaldehyde were purchased from Sigma Aldrich and used without further purification. $Ir(ppy)_3$, $Ir(ppy)_2(dtbbpy)[PF_6]$, $[Ir(dF(CF_3)ppy)_2(dtbbpy)]PF_6$, $[Ir(p\text{-}F(Me)ppy)_2(dtbbpy)]PF_6$ were purchased from Strem and used without further purification. $[TBA]NO_3$ was purchased from Alfa Aesar, and was dissolved in THF, filtered over activated alumina to dry to purify prior to use. $^{15}N_2$ was obtained from Cambridge Isotope Laboratories, Inc. (Lot number: I-25854/XZ732957). $^{15}NH_4Cl$ (99% ^{15}N, 98% purity) and $Na^{15}NO_3$ (98% ^{15}N, 98% purity) were purchased from Cambridge Isotope Laboratories, Inc. and used without further purification. Collidine was purchased from Sigma Aldrich and was distilled prior to use. 9,10-dihydroacridine (98%) was purchased from Combi Blocks and used without further purification. 1-benzyl-1,4-dihydronicotinamide was purchased from TCI and used without further purification. Acetylene (99.6% purity) was purchased from Matheson Gas. Tetrahydrofuran (THF) used in the experiments herein was stirred over Na/K ($\geq$ 12 hours) and filtered over activated alumina or vacuum-transferred before use unless otherwise stated.

Photoinduced reactions were performed using Kessil® 34 W 150 Blue lamps.

C.1.3 Physical Methods

NMR: Nuclear Magnetic Resonance (NMR) measurements were recorded with a Varian 400 MHz spectrometer. ^{1}H NMR chemical shifts are reported in ppm relative to tetramethylsilane, using ^{1}H resonances from residual solvent as internal standards.[10]

UV-Vis: Ultraviolet-visible (UV-vis) absorption spectroscopy measurements were collected with a Cary 50 UV-vis spectrophotometer using a 1 cm path length quartz cuvette. All samples had a blank sample background subtraction applied.

EPR Spectroscopy: All X-band continuous-wave electron paramagnetic resonance (CW-EPR) spectra were obtained on a Bruker EMX spectrometer using a quartz liquid nitrogen immersion dewar on solutions prepared as frozen glasses in 2-MeTHF.

Steady-state fluorimetry: Steady-state fluorimetry was performed in the Beckman Institute Laser Resource Center (BILRC; California Institute of Technology). Samples for luminescence measurements were prepared in dry THF and transferred to a 1-cm pathlength fused quartz cuvette sealed with a high-vacuum Teflon valve (Kontes). Steady-state emission spectra were collected on a Jobin S4 Yvon Spec Fluorolog-3-11 with a Hamamatsu R928P photomultiplier tube detector with photon counting.

C.1.4. Synthetic details

^{15}N-labelled 2,6-Dimethyl-3,5-dicarboethoxy-l,4-dihydropyridine (^{15}N-HEH$_2$).

Adapted from ref 1. Aqueous formaldehyde (37%, 78 μL) and ethyl acetoacetate (280 μL, 2.19 mmol) were placed in a 10 mL round-bottom flask equipped with a stir bar and fitted with a reflux condenser. $^{15}NH_4Cl$ (305 mg, 5.7 mmol) in 1 mL H_2O was added to a 1 mL aqueous solution of NaOH (228.3 mg, 5.7 mmol). The resulting solution of $^{15}NH_4OH$ was added to the flask through the neck of the condenser. The condenser neck was rinsed into the flask with 0.5 mL ethanol. The reaction mixture was heated at reflux for 1.5 hrs and then chilled in an ice bath. The resulting precipitate was collected by filtration and washed with cold ethanol (~3 mL) and Et_2O to yield the title compound as a pale yellow powder (60 mg, 22% yield). ^{1}H NMR (400 MHz, DMSO-d_6) δ 8.28 (d, $^{1}J_{H,N}$ =

94.6 Hz, 1H), 4.05 (q, J = 7.1 Hz, 4H), 3.11 (s, 2H), 2.11 (d, J = 2.9 Hz, 6H), 1.19 (t, J = 7.1 Hz, 6H) ppm.

^{15}N-labelled 2,4,6-Dimethylpyridinium (^{15}N-[ColH]OTf).

An identical procedure to what has previously been reported with unlabeled Col was employed.[2] ^{1}H NMR (400 MHz, DMSO-d_6) δ 14.87 (broad s, 1H), 7.57 (d, $^3J_{H,N}$ = 2.8 Hz, 2H), 2.62 (d, $^3J_{H,N}$ = 2.9 Hz, 6H), 2.49 (s, 3H) ppm.

[4,4′-Bis(1,1-dimethylethyl)-2,2′-bipyridine-N1,N1′]bis[2-(2-pyridinyl-N)phenyl-C]iridium(III) Tetrakis(3,5-bis(trifluoromethyl)phenyl)borate ([Ir]BAr$^F_4$).

Ir(ppy)$_2$(dtbbpy)[PF$_6$] (100 mg, 0.11 mmol) and Na[BAr$^F_4$] (92.2 mg, 0.10 mmol, 0.95 eq) were stirred in 5 mL Et$_2$O at room temperature for 1 hour. The solution was filtered through celite, layered with pentane, and stored at -40°C overnight to yield the title compound as yellow crystals (161 mg, 90% yield). ^{1}H NMR (400 MHz, MeCN-d_3) δ 8.48 (s, 2H), 8.06 (d, 2H, J = 8.2 Hz), 7.93-7.76 (m, 6H), 7.74-7.64 (m, 10H), 7.58 (d, J = 5.8 Hz, 2H), 7.50 (dd, J = 5.9, 1.9 Hz, 2H), 7.03 (t, J = 6.8 Hz, 2H), 6.91 (t, J = 6.8 Hz, 2H), 6.28 (d, J = 6.3 Hz, 2H), 1.40 (s, 18H) ppm.

C.2 NH$_3$ generation experiments

C.2.1 Standard NH$_3$ Generation Reaction Procedure

All solvents are stirred with Na/K for ≥2 hours and filtered prior to use. In a nitrogen-filled glovebox, the precatalysts ([MoBr$_3$] and/or [Ir]BAr$^F_4$) (2.3 μmol) are weighed in individual vials.* The precatalysts are then transferred quantitatively into a Schlenk tube using THF. The THF is then evaporated to provide a thin film of precatalyst at the bottom of the Schlenk tube. The tube is then charged with a stir bar and the acid and Hantzsch ester (HEH$_2$) are added as solids. The tube is cooled to 77 K in a cold well. The base ([Col]) is dissolved in 1 mL solvent. To the cold tube is added the 1 mL solution of base and solvent to produce a concentration of precatalyst of 2.3 mM. The temperature of the system is allowed to equilibrate for 5 minutes, and then the tube is sealed with a Teflon screw-valve. This tube is passed out of the box into a liquid N$_2$ bath and transported to a fume hood. For experiments run at -78 °C, the tube is then transferred to a dry ice/isopropanol bath, where it

thaws and is allowed to stir under blue LED irradiation at -78 °C for a minimum of three hours before warming. For experiments run at 23 °C, the tube is instead transferred to a water bath where it thaws and is allowed to stir for 12 hours. To ensure reproducibility, all experiments were conducted in 200 mL Schlenk tubes (50 mm OD) using 10 mm egg-shaped stir bars, and stirring was conducted at ~600 rpm. Both the water bath and the dry ice/isopropanol bath were contained in highly reflective dewars. The Blue LED was placed above the bath as close to the stirring reaction.

* In cases where less than 2.3 μmol of precatalyst were used, stock solutions were used to avoid having to weigh very small amounts.

C.2.2 NH_3 Generation Reaction Procedure under Partial H_2 Atmosphere

Catalytic runs done under a mixture of H_2 and N_2 were conducted similarly to those under N_2 atmosphere, with a few differences described below. The loadings were the same as in Table 4.1, Entry 10.

Catalysis is performed in the same Schlenk tubes as under N_2, which are charged with precatalyst, HEH_2, [ColH]OTf, and a stir bar in a nitrogen-filled glovebox as described above. After addition of the solids, the tube is wrapped in aluminum foil and the base (Col) is added in 1 mL of Na/K dried THF at room temperature. Half of the headspace volume is then removed using a calibrated bulb and then backfilled with H_2 which has been passed through a liquid nitrogen trap. The aluminum foil is removed, and the reaction is allowed to stir under Blue LED irradiation for 12 hours. Variation from the standard procedure (addition of THF/Col at room temperature and allowing to stir without irradiation for 30 min before exposing to blue LED) were found to not perturb the yield of NH_3.

C.2.3 NH_3 detection by optical methods

Reaction mixtures are cooled to 77 K and allowed to freeze. The reaction vessel is then opened to atmosphere and to the frozen solution an excess of a solution of HCl (3 mL of a 2.0 M solution in Et_2O, 6 mmol) is added over 1-2 minutes. This solution is allowed to freeze, then the headspace of the tube is evacuated, and the tube is sealed. The tube is then allowed to warm to RT and stirred at RT for at least 10 minutes. Solvent is removed *in vacuo*,

and the solids are extracted with 1 M HCl(aq) and filtered to give a total solution volume of 10 mL. A 5 mL aliquot is taken and washed repeatedly with n-butanol to remove Hantzsch pyridine (HE) and collidinium. After n-butanol washing additional 1 M HCl(aq) is added to give a final total volume of 5 mL. From these 5 mL solutions, a 100 µL aliquot is analyzed for the presence of NH_3 (present as $[NH_4][Cl]$) by the indophenol method. Quantification was performed with UV-vis spectroscopy by analyzing the absorbance at 635 nm.[11] When specified, a further aliquot of this solution was analyzed for the presence of N_2H_4 (present as $[N_2H_5][Cl]$) by a standard colorimetric method.[12] Quantification was performed with UV-vis spectroscopy by analyzing the absorbance at 458 nm.

C.2.4 NH_3 detection by ^1H NMR

Reaction mixtures are cooled to 77 K and allowed to freeze. The reaction vessel is then opened to atmosphere and to the frozen solution an excess (with respect to acid) NaO^tBu solution in MeOH (0.25 mM) is added over 1-2 minutes. This solution is allowed to freeze, then the headspace of the tube is evacuated, and the tube is sealed. The tube is then allowed to warm to RT and stirred at RT for at least 10 minutes. An additional Schlenk tube is charged with HCl (3 mL of a 2.0 M solution in Et_2O, 6 mmol) to serve as a collection flask. The volatiles of the reaction mixture are vacuum transferred at RT into this collection flask. After completion of the vacuum transfer, the collection flask is sealed and warmed to RT. Solvent is removed in vacuo, and the remaining residue is dissolved in 0.7 mL of DMSO-d_6 containing 20 mM 1,3,5-trimethoxybenzene as an internal standard. Integration of the ^1H NMR peak observed for NH_4^+ is then integrated against the two peaks of trimethoxybenzene to quantify the ammonium present. This ^1H NMR detection method was also used to differentiate $[^{14}NH_4][Cl]$ and $[^{15}NH_4][Cl]$ produced in the control reactions conducted with $^{15}N_2$, ^{15}N-Col/[ColH]OTf, or ^{15}N-HEH_2.

C.2.5 NH_3 detection results

C.2.5.1 Catalytic results in main text (Table 4.1)

Table C.1: Catalytic yields for photodriven transfer hydrogenation of N_2 to NH_3.

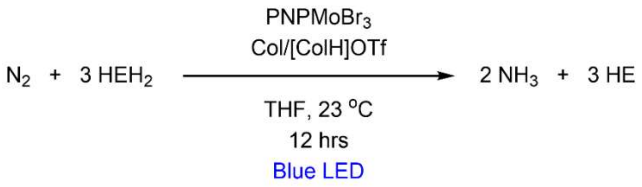

Run	Conditions	[Mo] load (µmol)	acid (µmol)	base (µmol)	Ir (µmol)	HEH_2 equiv /Mo	NH_3 equiv /Mo	N_2H_4 equiv/ Mo	NH_3 yield/ HEH_2 (%)
Table 4.1, entry 1: Standard conditions									
A1	THF, 23 °C	2.3	124.2	124.2	0	54	9.5	-	
B1	THF, 23 °C	2.3	124.2	124.2	0	54	8.3	-	
C1	THF, 23 °C	2.3	124.2	124.2	0	54	10.8	-	
	THF, 23 °C	2.3	124.2	124.2	0	54	9.5±1		26.5±3
Table 4.1, entry 2: 0.575 mM [$MoBr_3$]									
D1	THF, 23 °C	0.575	124.2	124.2	0	216	22.6	-	
E1	THF, 23 °C	0.575	124.2	124.2	0	216	20.9	-	
	THF, 23 °C	0.575	124.2	124.2	0	216	21.8±0.8		15.1±06
Table 4.1, entry 3: No Mo									
F1	THF, 23 °C	0	124.2	124.2	0	54	<0.1	<0.1	
G1	THF, 23 °C	0	124.2	124.2	0	54	<0.1	<0.1	
	THF, 23 °C	2.3	124.2	124.2	0	54	<0.1	<0.1	<0.3
Table 4.1, entry 4: No light									
H1	THF, 23 °C no light	2.3	124.2	124.2	0	54	<0.1	<0.1	
I1	THF, 23 °C no light	2.3	124.2	124.2	0	54	<0.1	<0.1	
	THF, 23 °C no light	2.3	124.2	124.2	0	54	<0.1	<0.1	<0.3
Table 4.1, entry 5: No buffer									
J1	THF, 23 °C	2.3	**0**	**0**	0	54	0.74	-	
K1	THF, 23 °C	2.3	**0**	**0**	0	54	1.11	-	
	THF, 23 °C	2.3	**0**	**0**	0	54	0.9±0.2		2.6±0.5
Table 4.1, entry 6: 5 equiv Col/[ColH]OTf									
L1	THF, 23 °C	2.3	11.5	11.5	0	54	2.7	<0.1	
M1	THF, 23 °C	2.3	11.5	11.5	0	54	3.2	<0.1	
N1	THF, 23 °C	2.3	11.5	11.5	0	54	2.8	-	
	THF, 23 °C	2.3	11.5	11.5	0	54	2.9±0.2	<0.1	8.1±0.6
Table 4.1, entry 7: benzene instead of THF									
O1	C_6H_6, 23 °C	2.3	124.2	124.2	0	54	4.8	-	
P1	C_6H_6, 23 °C	2.3	124.2	124.2	0	54	4.6	-	
	C_6H_6, 23 °C	2.3	124.2	124.2	0	54	4.7±0.1		13±0.3

Run	Conditions	[Mo] load (μmol	acid (μmol)	base (μmol)	Ir (μmol)	HEH_2 equiv /Mo	NH_3 equiv /Mo	N_2H_4 equiv/ Mo	NH_3 yield/ HEH_2 (%)
Table 4.1, entry 8: 216 equiv Col/[ColH]OTf									
Q1	THF, 23 °C	2.3	496.8	496.8	0	54	19.5	-	
R1	THF, 23 °C	2.3	496.8	496.8	0	54	21.1	-	
	THF, 23 °C	2.3	496.8	496.8	0	54	20.3±0.8		56±2
Table 4.1, entry 9: with 10 equiv TBABr									
S1	THF, 23 °C	2.3	124.2	124.2	0	54	9	-	
T1	THF, 23 °C	2.3	124.2	124.2	0	54	8.6	-	
	THF, 23 °C	2.3	124.2	124.2	0	54	8.8±0.3		23.6±0.8
Table 4.1, entry 10: Added [Ir]BAr^F_4									
U1	THF, 23 °C	2.3	124.2	124.2	2.3	54	29.8	-	
V1	THF, 23 °C	2.3	124.2	124.2	2.3	54	20.6	-	
W1	THF, 23 °C	2.3	124.2	124.2	2.3	54	20.5	-	
X1	THF, 23 °C	2.3	124.2	124.2	2.3	54	25.4	-	
	THF, 23 °C	2.3	124.2	124.2	2.3	54	24±4		67±10
Table 4.1, entry 11: Added [Ir]BAr^F_4, 5 equiv Col/[ColH]OTf									
Y1	THF, 23 °C	2.3	11.5	11.5	2.3	54	16.02	<0.1	
Z1	THF, 23 °C	2.3	11.5	11.5	2.3	54	16.6	<0.1	
AA1	THF, 23 °C	2.3	11.5	11.5	2.3	54	14.7		
	THF, 23 °C	2.3	11.5	11.5	2.3	54	15.8±0.8	<0.1	44±2
Table 4.1, entry 12: Added [Ir]BAr^F_4, t = ½ h									
AB1	THF, 23 °C t = ½ h	2.3	124.2	124.2	2.3	54	19.5	-	
AC1	THF, 23 °C t = ½ h	2.3	124.2	124.2	2.3	54	17.7	-	
	THF, 23 °C t = 1/2 h	2.3	124.2	124.2	2.3	54	18.6±0.9		52±3
~75 % completion compared to entry 10									
Table 4.1, entry 13: t = 2 h									
AD1	THF, 23 °C t = 2 h	2.3	124.2	124.2	0	54	4.9	-	
AE1	THF, 23 °C t = 2 h	2.3	124.2	124.2	0	54	7.9	-	
AF1	THF, 23 °C t = 2 h	2.3	124.2	124.2	0	54	10	-	
	THF, 23 °C t = 2 h	2.3	124.2	124.2	0	54	7.6±2		21±6
~80 % completion compared to entry 1									
Table 4.1, entry 14: Added [Ir]BAr^F_4, 5 equiv Col/[ColH]OTf, 0.575 mM [$MoBr_3$]									
AG1	THF, 23 °C	0.575	11.5	11.5	2.3	216	26.83	-	
AH1	THF, 23 °C	0.575	11.5	11.5	2.3	216	25.96	-	
	THF, 23 °C	0.575	11.5	11.5	2.3	216	26±0.4		18.4±0.4
Table 4.1, entry 15: Added [Ir]BAr^F_4, 5 equiv Col/[ColH]OTf, no light									
AI1	THF, 23 °C no light	2.3	11.5	11.5	2.3	54	<0.1	<0.1	
AJ1	THF, 23 °C no light	2.3	11.5	11.5	2.3	54	<0.1	<0.1	
	THF, 23 °C no light	2.3	11.5	11.5	2.3	54	<0.1	<0.1	<0.3

Run	Conditions	[Mo] load (μmol	acid (μmol)	base (μmol)	Ir (μmol)	HEH_2 equiv /Mo	NH_3 equiv /Mo	N_2H_4 equiv /Mo	NH_3 yield/ HEH_2 (%)
Table 4.1, entry 16: Added [Ir]BAr^F_4, 5 equiv Col/[ColH]OTf, no [$MoBr_3$]									
AK1	THF, 23 °C	**0**	11.5	11.5	2.3	54	<0.1	<0.1	
AL1	THF, 23 °C	**0**	11.5	11.5	2.3	54	<0.1	<0.1	
	THF, 23 °C	**0**	11.5	11.5	2.3	54	<0.1	<0.1	<0.3
Table 4.1, entry 17: Added [Ir]BAr^F_4, 5 equiv Col/[ColH]OTf, no HEH_2									
AM1	THF, 23 °C	2.3	11.5	11.5	2.3	**0**	<0.1	<0.1	
AN1	THF, 23 °C	2.3	11.5	11.5	2.3	**0**	<0.1	<0.1	
	THF, 23 °C	2.3	11.5	11.5	2.3	**0**	<0.1	<0.1	<0.3
Table 4.1, entry 18: Added [Ir]BAr^F_4, subH_2 = 9,10-dihydroacridine									
AO1	THF, 23 °C	2.3	124.2	124.2	2.3	54[a]	6.7	-	
AP1	THF, 23 °C	2.3	124.2	124.2	2.3	54[a]	6.1	-	
	THF, 23 °C	2.3	124.2	124.2	2.3	54[a]	6.4±0.3		17.7±0.8
[a]9,10-dihydroacridine used instead of HEH_2									
Table 4.1, entry 19: Added [Ir]BAr^F_4, subH_2 = 5,6-dihydrophenanthridine									
AQ1	THF, 23 °C	2.3	124.2	124.2	2.3	54[b]	4.5	-	
AR1	THF, 23 °C	2.3	124.2	124.2	2.3	54[b]	5.1	-	
	THF, 23 °C	2.3	124.2	124.2	2.3	54[b]	4.6±0.8		13±2
[b]5,6-dihydrophenanthridine used instead of HEH_2									
Table 4.1, entry 20: Added [Ir]BAr^F_4, subH_2 = 1-benzyl-1,4-dihydronicotinamide									
AS1	THF, 23 °C	2.3	124.2	124.2	2.3	54[c]	1.31	-	
AT1	THF, 23 °C	2.3	124.2	124.2	2.3	54[c]	1.12	-	
	THF, 23 °C	2.3	124.2	124.2	2.3	54[c]	1.2±0.1		3.3±0.3
[c]1-benzyl-1,4-dihydronicotinamide used instead of HEH_2									
Table 4.1, entry 21: Added [Ir]BAr^F_4, 0.5 atm H_2, 0.5 atm N_2									
AU1	THF, 23 °C $P_{N2} = P_{H2}$ = 0.5 atm	2.3	124.2	124.2	2.3	54	16.1	-	
AV1	THF, 23 °C $P_{N2} = P_{H2}$ = 0.5 atm	2.3	124.2	124.2	2.3	54	11.0	-	
	THF, 23 °C $P_{N2} = P_{H2}$ = 0.5 atm	2.3	124.2	124.2	2.3	54	14±4		36±9
Table 4.1, entry 22: Added [Ir(dF(CF_3)ppy)$_2$(dtbbpy)]PF_6 , t = 2 h									
AW1	THF, 23 °C t = 2 h	2.3	124.2	124.2	2.3	54	1.8	-	
AX1	THF, 23 °C t = 2 h	2.3	124.2	124.2	2.3	54	2.6	-	
	THF, 23 °C t = 2 h	2.3	124.2	124.2	2.3	54	2.2±0.6		6±1
Table 4.1, entry 23: Added [Ir]PF_6, t = 2 h									
AY1	THF, 23 °C t = 2 h	2.3	124.2	124.2	2.3	54	18.4	-	
AZ1	THF, 23 °C t = 2 h	2.3	124.2	124.2	2.3	54	23.5	-	
	THF, 23 °C t = 2 h	2.3	124.2	124.2	2.3	54	21±4		58±10
Table 4.1, entry 24: Added [Ir(*p*-F(Me)ppy)$_2$(dtbbpy)]PF_6 , t = 2 h									

Run	Conditions	[Mo] load (μmol	acid (μmol)	base (μmol)	Ir (μmol)	HEH_2 equiv /Mo	NH_3 equiv /Mo	N_2H_4 equiv/Mo	NH_3 yield/ HEH_2 (%)
BA1	THF, 23 °C t = 2 h	2.3	124.2	124.2	2.3	54	21.5	-	
BB1	THF, 23 °C t = 2 h	2.3	124.2	124.2	2.3	54	23.1	-	
	THF, 23 °C t = 2 h	2.3	124.2	124.2	2.3	54	22±1		62±3

Table 4.1, entry 25: Added $Ir(ppy)_3$, t = 2 h

BC1	THF, 23 °C t = 2 h	2.3	124.2	124.2	2.3	54	7.8	-	
BD1	THF, 23 °C t = 2 h	2.3	124.2	124.2	2.3	54	5.8	-	
	THF, 23 °C t = 2 h	2.3	124.2	124.2	2.3	54	7±1		19±4

Table 4.1, entry 26: Added [Ir]BAr^F_4, no Col/[ColH]OTf

BE1	THF, 23 °C t = 2 h	2.3	124.2	124.2	2.3	54	7.03	-	
BF1	THF, 23 °C t = 2 h	2.3	124.2	124.2	2.3	54	7.83	-	
	THF, 23 °C t = 2 h	2.3	124.2	124.2	2.3	54	7.4±0.4		20.7±1

C.2.5.2 Additional catalytic experiments

Table C.2: Canvassing H_2 carriers

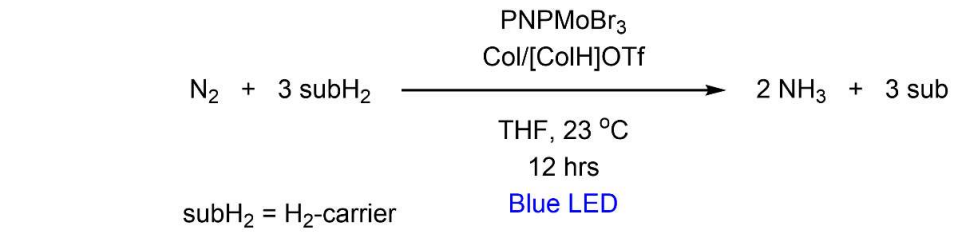

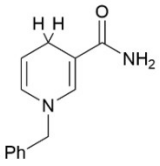

BNAH
(1-benzyl-1,4-dihydronicotinamide)

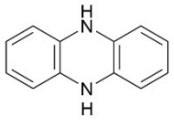

$phenazH_2$
(5,10-dihydrophenazine)

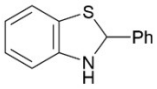

BTH_2
(2-phenylbenzothiazolin)

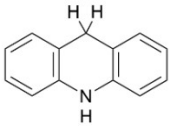

$acrH_2$
(9,10-dihydroacridine)

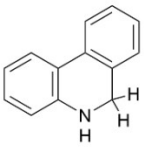

$phenH_2$
(5,6-dihydrophenanthridine)

Run	subH₂	[MoBr₃] load (µmol)	acid (µmol)	base (µmol)	Ir (µmol)	subH₂ equiv /Mo	NH₃ equiv /Mo	N₂H₄ equiv/Mo	NH₃ yield/ subH₂ (%)
A2	BNAH	2.3	124.2	124.2	**0**	54	0.55	-	
B2	BNAH	2.3	124.2	124.2	**0**	54	0.30	-	
	BNAH	2.3	124.2	124.2	**0**	54	0.4±0.1		1.2±0.3
C2	$PhenazH_2$	2.3	124.2	124.2	**2.3**	54	<0.1	-	
D2	$PhenazH_2$	2.3	124.2	124.2	**2.3**	54	<0.1	-	
	$PhenazH_2$	2.3	124.2	124.2	**2.3**	54	<0.1		<0.1
E2	BTH_2	2.3	124.2	124.2	**2.3**	54	<0.1	-	
F2	BTH_2	2.3	124.2	124.2	**2.3**	54	<0.1	-	
	BTH_2	2.3	124.2	124.2	**2.3**	54	<0.1		<0.1
G2	$AcrH_2$	2.3	124.2	124.2	**0**	54	0.09	-	
H2	$AcrH_2$	2.3	124.2	124.2	**0**	54	0.24	-	
	$AcrH_2$	2.3	124.2	124.2	**0**	54	0.16±0.08		0.5±0.2
I2	$PhenH_2$	2.3	124.2	124.2	**0**	54	0.216	-	
J2	$PhenH_2$	2.3	124.2	124.2	**0**	54	0.205	-	
	$PhenH_2$	2.3	124.2	124.2	**0**	54	0.211±0.008		0.66±0.02

Table C.3. Additional time course experiments.

Run	Conditions	Mo loading (μmol)	acid (μmol)	base (μmol)	Ir (μmol)	HEH_2 equiv /Mo	NH_3 equiv /Mo	N_2H_4 equiv/Mo	NH_3 yield/ HEH_2 (%)
A3	THF, 23 °C t = 2 h	2.3	124.2	124.2	2.3	54	24.5	-	
B3	THF, 23 °C t = 2 h	2.3	124.2	124.2	2.3	54	25.5	-	
	THF, 23 °C t = 2 hours	2.3	124.2	124.2	2.3	54	25±0.5		69.4±1.5
Approximately 100% completion compared to Table 4.1, entry 10									
C3	THF, rt, 10 min	2.3	124.2	124.2	2.3	54	8.2	-	22.8
Approximately 30% completion compared to Table 4.1, entry 10									

Table C.4 Catalysis using [ColH]OTf or Col instead of buffered solution

Run	Conditions	Mo loading (μmol)	acid (μmol)	base (μmol)	Ir (μmol)	HEH_2 equiv /Mo	NH_3 equiv /Mo	N_2H_4 equiv/Mo	NH_3 yield/ HEH_2 (%)
A4	THF, 23°C	2.3	496.8	**0**	**0**	54	5.8	-	
B4	THF, 23°C	2.3	496.8	**0**	**0**	54	5.5	-	
	THF, 23°C	2.3	496.8	**0**	**0**	54	5.65±.15		15.7±0.4
C4	THF, 23°C	2.3	**0**	496.8	**0**	54	1.2	-	
D4	THF, 23°C	2.3	**0**	496.8	**0**	54	2.0	-	
	THF, 23°C	2.3	**0**	496.8	**0**	54	1.6±0.4		4.7±1.1

Table C.5. Solvent screen

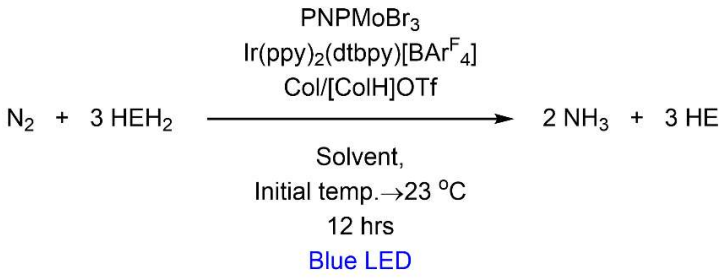

Run	Conditions	Mo loading (µmol)	acid (µmol)	base (µmol)	Ir (µmol)	HEH_2 equiv /Mo	NH_3 equiv /Mo	N_2H_4 equiv/Mo	NH_3 yield/ HEH_2 (%)
A5	THF, -78 →23°C	2.3	11.5	11.5	2.3	54	15.47	-	
B5	THF, -78 →23°C	2.3	11.5	11.5	2.3	54	16.06	-	
	THF, -78 →23°C	2.3	11.5	11.5	2.3	54	15.7±0.3		44.8±0.8
C5	Tol, 23°C	2.3	11.5	11.5	2.3	54	7	-	
D5	Tol, 23°C	2.3	11.5	11.5	2.3	54	7.3	-	
	Tol 23°C	2.3	11.5	11.5	2.3	54	7.15±0.15		19.8±0.8
E5	Tol, -78 →23°C	2.3	11.5	11.5	2.3	54	13.01	-	
F5	Tol, -78 →23°C	2.3	11.5	11.5	2.3	54	14.24	-	
	Tol, -78 →23°C	2.3	11.5	11.5	2.3	54	13.6±0.6		38±2
G5	Et_2O, -78 →23°C	2.3	11.5	11.5	2.3	54	4.08	-	
H5	Et_2O, -78 → 23°C	2.3	11.5	11.5	2.3	54	3.97	-	
	Et_2O, -78 → 23°C	2.3	11.5	11.5	2.3	54	4.0±0.1		11.2±0.2
I5	THF, -78 →23°C	2.3	11.5	11.5	2.3[a]	54	7.4	-	
J5	THF, -78 →23°C	2.3	11.5	11.5	2.3[a]	54	11.7	-	
	THF, -78 →23°C	2.3	11.5	11.5	2.3[a]	54	9.6±2		27±7
K5	MeCy, 23°C	2.3	124.2	124.2	0	54	<0.1	-	
L5	MeCy, 23°C	2.3	124.2	124.2	0	54	<0.1	-	
	MeCy, 23°C						<0.1		<0.3

[a]$Ir(ppy)_3$ used as photosensitizer
Tol = toluene; MeCy = methylcyclohexane

Solubility of reagents:
Collidine: Soluble in THF, Et_2O, Toluene, C_6H_6, MeCy
Collidinium triflate: Soluble in THF, insoluble in Et_2O, Toluene and C_6H_6, MeCy

[$MoBr_3$]: Soluble in THF, Toluene and C_6H_6. Sparingly soluble in Et_2O, MeCy
HEH_2: Partially soluble in THF, Et_2O, Toluene and C_6H_6. Most soluble in THF, MeCy
[Ir]BAr^F_4: Soluble in THF, Et_2O, partially soluble in C_6H_6 and Toluene

Table C.6 Attempted catalysis with [P_3^BFe]BAr^F_4

Run	Conditions	Fe loading (µmol)	acid (µmol)	base (µmol)	Ir (µmol)	HEH_2 equiv /Fe	NH_3 equiv /Fe	N_2H_4 equiv/Fe	NH_3 yield/ HEH_2 (%)
A6	THF, 23°C	2.3	124.2	124.2	2.3	54	<0.1	<0.1	
B6	THF, 23°C	2.3	124.2	124.2	2.3	54	<0.1	<0.1	
	THF, 23°C	2.3	124.2	124.2	2.3	54	<0.1	<0.1	<0.1
C6	THF, 23°C	2.3	124.2	124.2	0	54	<0.1	<0.1	
D6	THF, 23°C	2.3	124.2	124.2	0	54	<0.1	<0.1	
	THF, 23°C	2.3	124.2	124.2	0	54	<0.1	<0.1	<0.1

C.2.6 NH_3 detection results from ^{15}N-HEH_2, ^{15}N-Col/^{15}N-[ColH]OTf and $^{15}N_2$ experiments

C.2.6.1 $^{15}N_2$ experiments

Catalytic runs done under a $^{15}N_2$ atmosphere were conducted similarly to those under a $^{14}N_2$ atmosphere, with a few differences described below. The loadings were the same as in Table 4.1, Entry 1.

Catalysis is performed in the same catalytic tubes as natural abundance experiments, which are charged with precatalyst, HEH_2, [ColH]OTf, and a stir bar in a nitrogen-filled glovebox, as described above. After addition of the solids, the tube is then cooled to 77 K in a cold well. The base (Col) is added by micropipette to the frozen tube by opening the Kontes. The Kontes was closed, and the tube was kept frozen, then passed out of the glovebox into a liquid N_2 bath. The headspace of the tube is evacuated while still submerged in liquid N_2.

Na/K dried THF is filtered, and 1 mL is placed into a separate Schlenk tube. The solvent undergoes freeze-pump thaw cycles (3 cycles) and is then vacuum transferred into the catalysis tube. This tube is allowed to warm up briefly and charged with $^{15}N_2$ via a vacuum bridge. The tube is refrozen at 77 K and then transferred to a water bath, where it thaws and is allowed to stir under Blue LED irradiation for 12 hours.

C.6.2 ^{15}N-HEH$_2$, ^{15}N-Col/^{15}N-[ColH]OTf experiments

Catalytic runs were set-up as described in **C.2.1** but using either ^{15}N-HEH$_2$ as H$_2$-carrier or ^{15}N-Col/[ColH]OTf as buffer using the same conditions as Table 4.1, Entry 1.

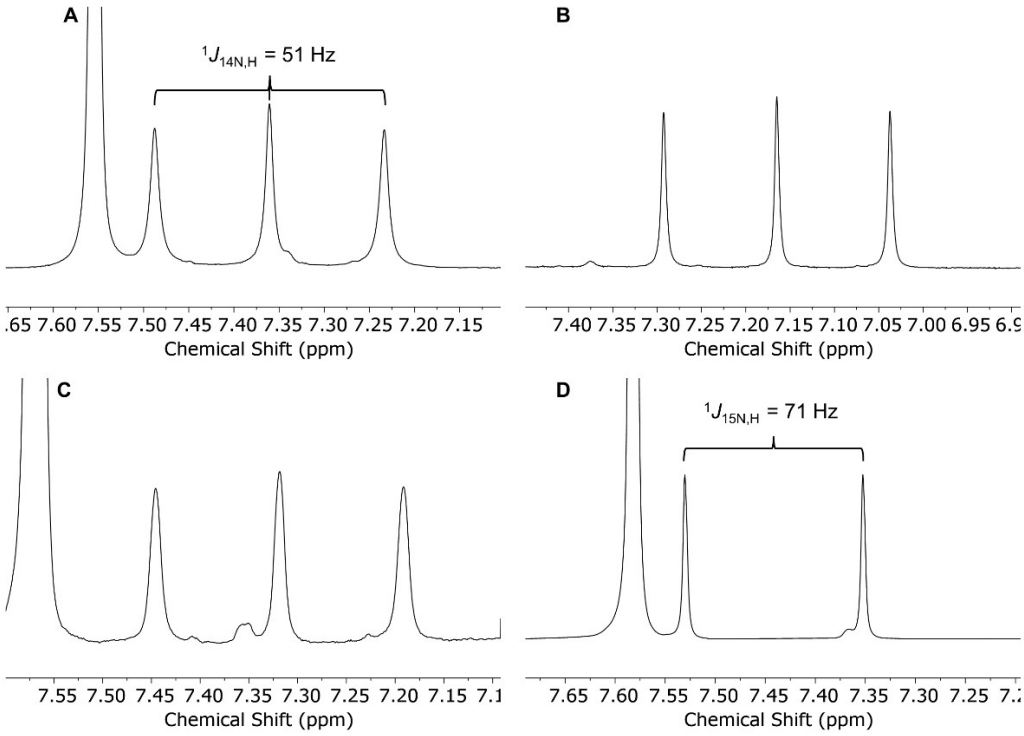

Figure C.1. ^{1}H NMR (DMSO-d_6, 400 MHz) of: A) ^{14}NH$_4$Cl obtained from reaction of natural abundance reactants under ^{14}N$_2$ (Ir-free conditions in Table 4.1, entry 1); B) ^{14}NH$_4$Cl obtained from reaction of ^{15}N-labeled HEH$_2$ (otherwise natural abundance reactants) under ^{14}N$_2$ (Ir-free conditions in Table 4.1, entry 1); C) ^{14}NH$_4$Cl obtained from reaction of ^{15}N-labeled Col/[ColH]OTf (otherwise natural abundance reactants) under ^{14}N$_2$ (Ir-free conditions in Table 4.1, entry 1); D) ^{15}NH$_4$Cl obtained from reaction under ^{15}N$_2$ (otherwise natural abundance reactants, Ir-free conditions in Table 4.1, entry 1).

C.2.7 Analysis of non-NH$_3$ catalysis products

After a complete catalytic run, instead of quenching the reaction (with acid or base) the solvent from the reaction mixture was removed *in vacuo*. The resulting film was taken up in minimal DMSO-d_6 and analyzed by NMR.

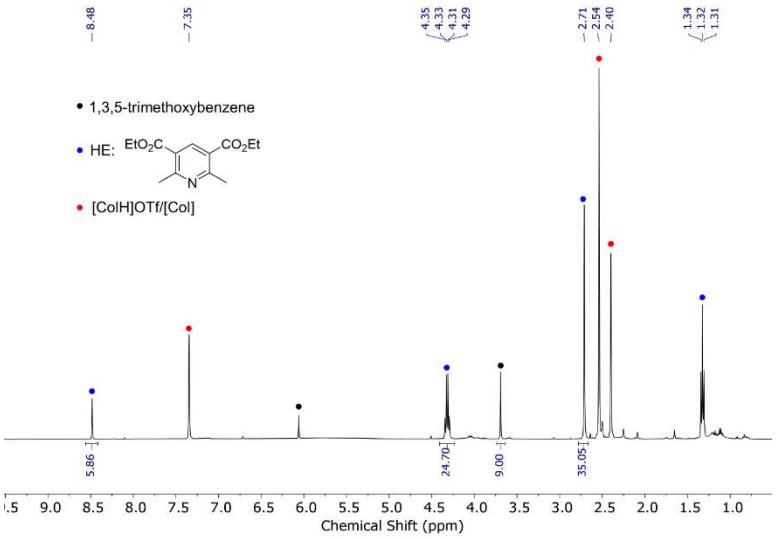

Figure C.2. ^{1}H NMR (DMSO-d_6, 400 MHz) of the nonvolatile products of the Mo-catalyzed reaction of HEH_2, [ColH]OTf, [Col], and N_2 under blue LED irradiation (Table 4,1, entry 1).

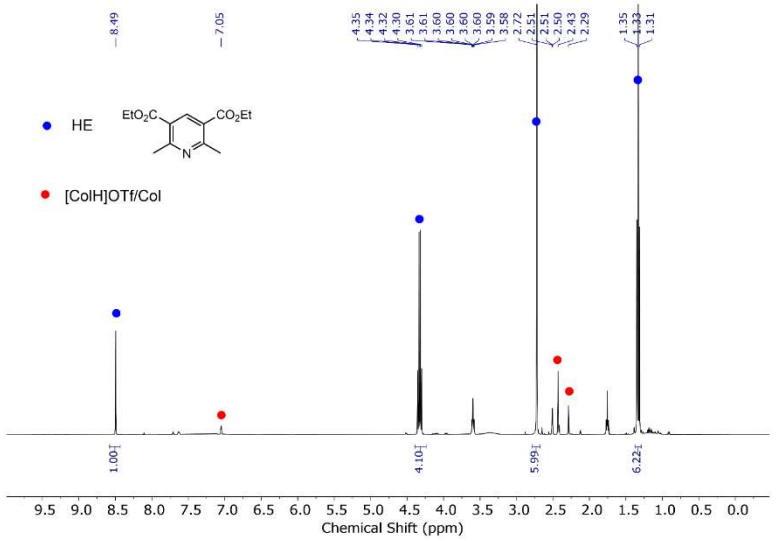

Figure C.3. ^{1}H NMR (DMSO-d_6, 400 MHz) of the nonvolatile products of the Col/[ColH]OTf-, Ir- and Mo-catalyzed reaction of HEH_2 and N_2 under blue LED irradiation (Table 4.1, entry 11, catalytic buffer).

C.2.8 ^{1}H NMR time course experiments

Procedure: A J.Young NMR tube was loaded with [$MoBr_3$], HEH_2, [ColH]OTf, Col, and N_2 and irradiated under blue LED. Conditions (concentration, temperature) were the

same as in Table 4.1, entry 1, but using THF-d_8 as solvent. Slightly slower reaction times are attributed to less efficient illumination and lack of stirring in the NMR tube compared to Schlenk flasks.

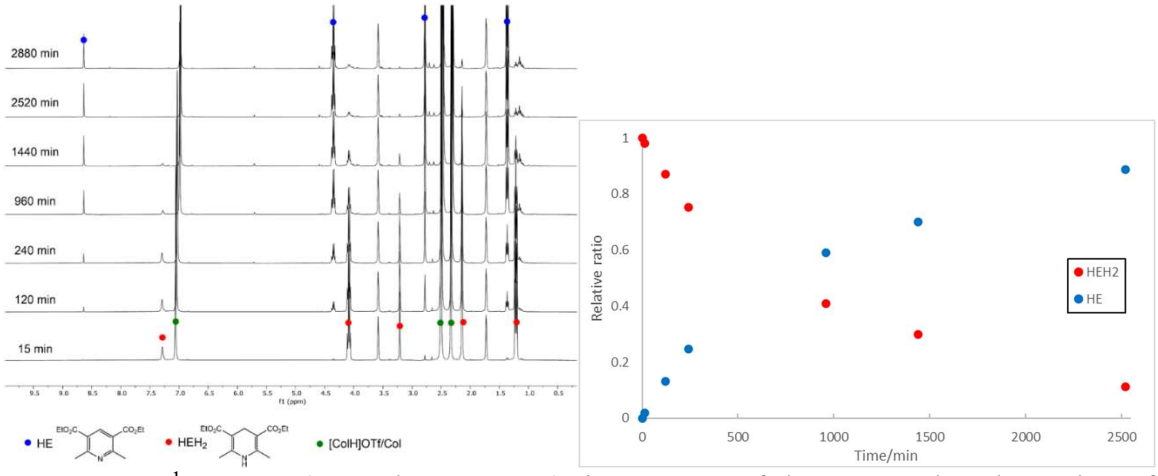

Figure C.4. ^{1}H NMR (THF-d_8, 400 MHz) time course of the Mo-catalyzed reaction of HEH_2, [ColH]OTf, Col, and N_2 under blue LED irradiation in a J. Young tube (Table 4.1 entry 1) (left). Relative ratio of HE and HEH_2 plotted over time (right).

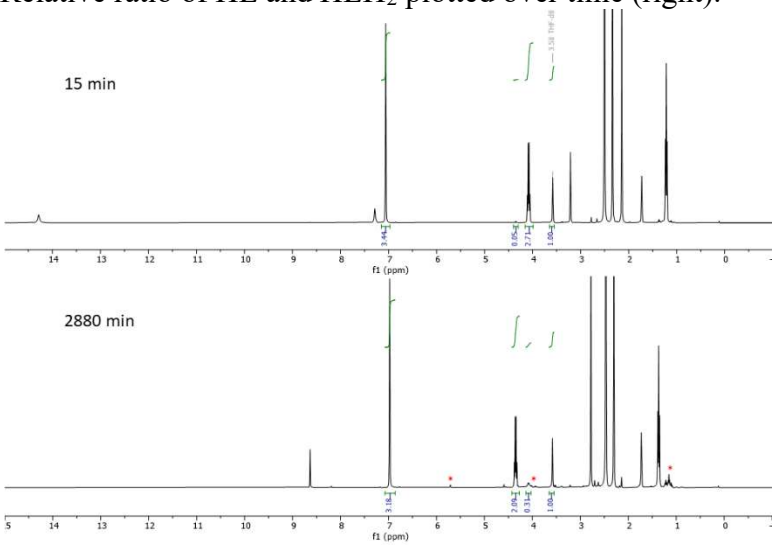

Figure C.5. ^{1}H NMR (THF-d_8, 400 MHz) of 15 minutes and 48 hour time points of the reaction of the Mo-catalyzed reaction of HEH_2, [ColH]OTf, Col, and N_2 under blue LED irradiation in a J.Young tube (Figure C.4). Integrals of HEH_2 and HE quartet peak at ~ 4.0 ppm are compared to constant THF solvent residual peaks to estimate total recovery of HEH_2 and HE. Approx. 90% is recovered. Similarly, integrals of Col/[ColH]OTf aromatic peak at ~ 7.0 ppm are compared to constant THF solvent residual peaks to estimate total recovery of Col/[ColH]OTf. Approx. 90% is recovered. *indicates minor organic impurity that grows in, see Figure C.6.

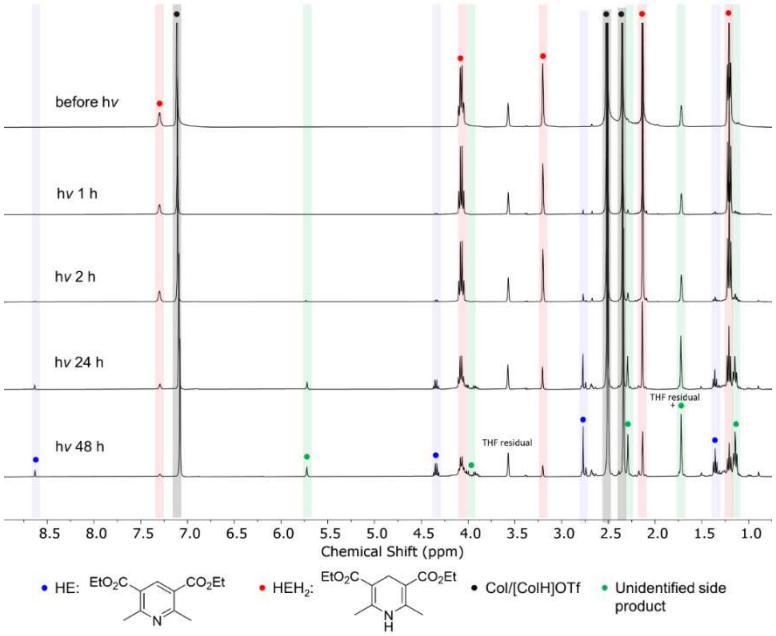

Figure C.6. ^{1}H NMR (THF-d_8, 400 MHz) before irradiation and at indicated timepoints following blue LED irradiation of the reaction of HEH_2 with 1 equiv Col and 1 equiv [ColH]OTf in a J. Young tube. Integration relative to the THF residual peak at 3.58 ppm indicates that after 48 hours, 79% of HEH_2 and 10% of the total initial buffer loading are consumed, while HE is produced in 16% conversion along with the same major organic side product peaks observed in N_2R with [$MoBr_3$] (Figure C.4 and C.5).

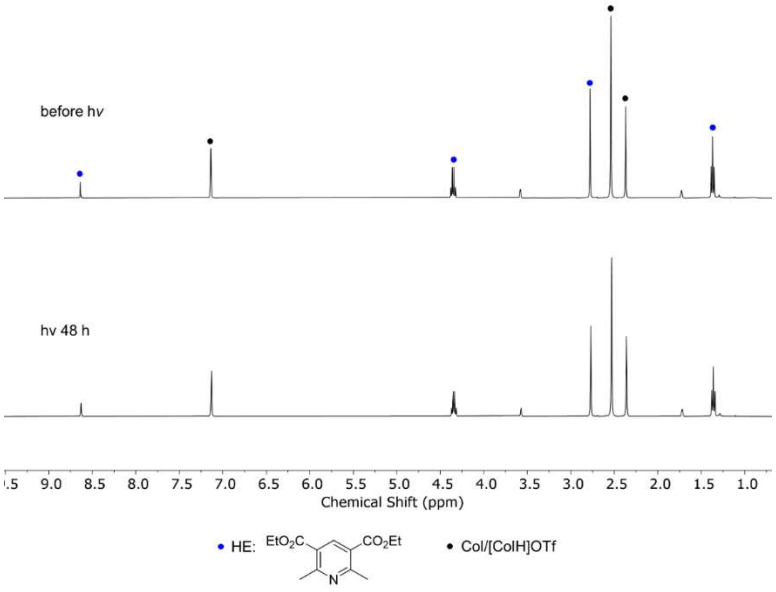

Figure C.7. ^{1}H NMR (THF-d_8, 400 MHz) before irradiation and at indicated timepoints following blue LED irradiation of HE with 1 equiv Col and 1 equiv [ColH]OTf in a J. Young tube. No reaction is observed.

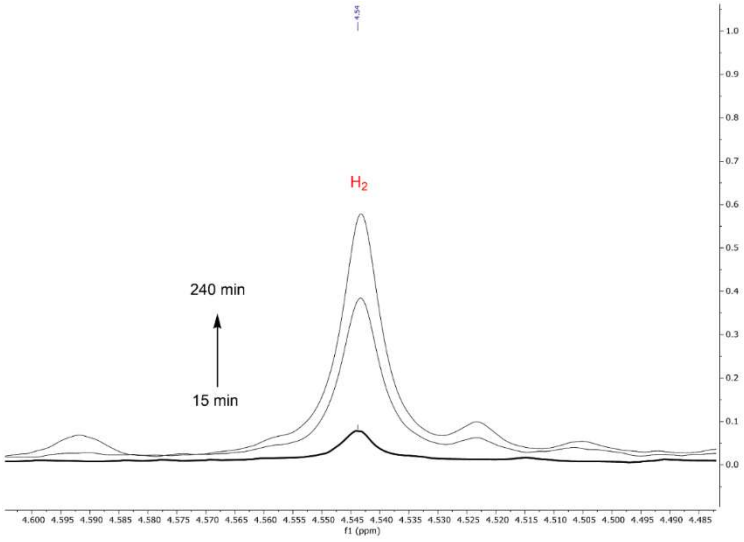

Figure C.8. ^{1}H NMR (THF-d_8, 400 MHz) of 15 minutes to 240 min of the Mo-catalyzed reaction of HEH_2, [ColH]OTf, Col, and N_2 under blue LED irradiation in a J.Young tube (Figure C.4). The H_2 peak (4.54 ppm)[10] grows in over time.

C.3 Steady-State Fluorescence Measurements

C.3.1 Procedure for Fluorimetry Studies

1 cm quartz glass cuvettes were loaded with 0.5 mM HEH_2 solutions in dry THF, with varying concentrations of quencher (either Col or [ColH]OTf) in a nitrogen glovebox. Stock solutions were used to assure consistency. Solutions were excited at 390 nm wavelength to avoid interference of the excitation wavelength and steady-state fluorescence spectra. Experiments were conducted at 23 °C.

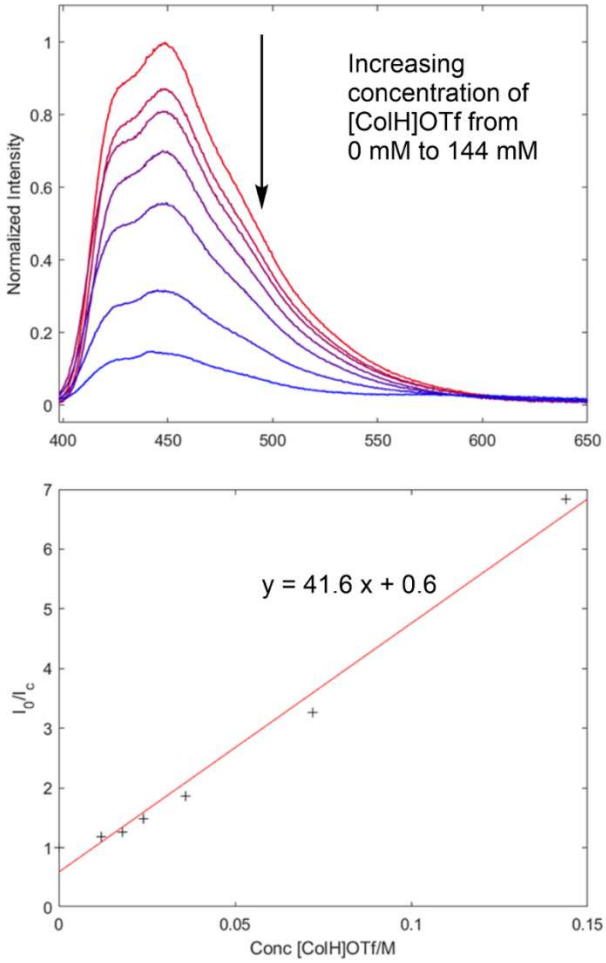

Figure C.9. Steady-state fluorescence of HEH_2 (0.5 mM) with varying amounts of [ColH]OTf (18 mM to 144 mM) (Top). Stern-Vollmer quenching plot of I_0/I_C against concentration of [ColH]OTf (bottom). Slope is 42±2.4 M^{-1}; R^2 =0.98.

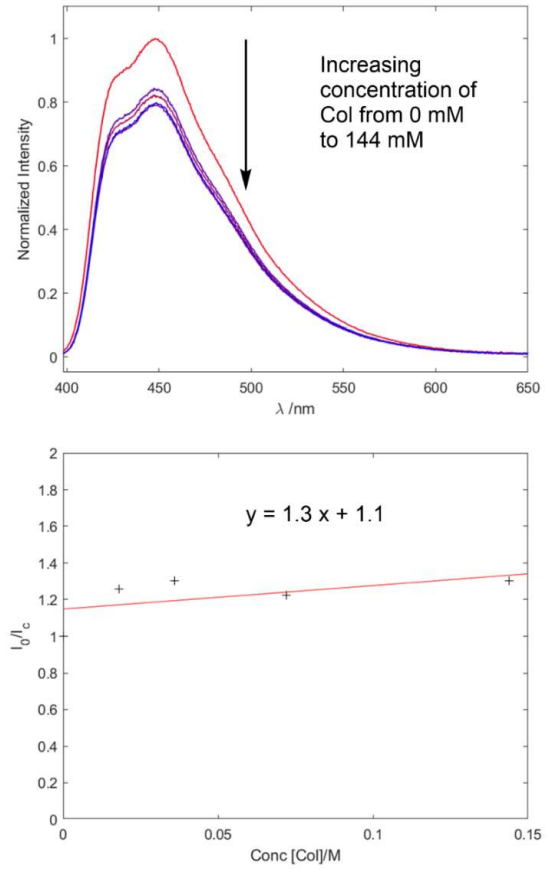

Figure C.10. Steady-state fluorescence of HEH_2 (0.5 mM) with varying amounts of Col (18 mM to 144 mM) (Top). Stern-Vollmer quenching plot of I_0/I_C against concentration of Col (bottom). Slope is 1.3±0.9 M^{-1}.

C.3.2 Calculation of Stern-Volmer quenching constants

Using the previously measured excited state-lifetime measured (τ_0) for HEH_2 we can calculate the Stern-Vollmer quenching lifetime using the equation:

$$I_0/I_c = 1 + k_q \cdot \tau_0 [Q] \text{ (eqn C.1)}$$

$$k_q = \text{slope}/\tau_0 \text{ (eqn C.2)}$$

While τ_0 has not been measured in THF at 25 °C, the measurements in DMSO at 25 °C (0.419 ns) provide a useful estimate.[17] Accordingly, the quenching constants are:

$$k_{colH} = 1.0 \pm 0.1 \cdot 10^{11}\ M^{-1}\ s^{-1}$$

$$k_{col} = 3 \pm 2 \cdot 10^{9}\ M^{-1}\ s^{-1}$$

While these values have considerable errors, particularly the Col quenching, these nonetheless provide useful order of magnitude estimates. The large rate constant for k_{colH+} suggests the presence of static quenching pathways.

C.4 UV-visible measurements

C.4.1 Procedure for UV-vis measurements.

1 cm quartz glass cuvettes were loaded with 0.1 mM HEH_2 solutions in dry THF inside the glovebox. The cuvette was taken out of the glovebox, and spectra were collected. Concentrated (50 mM) solutions of Col or [ColH]OTf were titrated into the cuvettes. The Col or [ColH]OTf solutions had 0.1 mM HEH_2 added to maintain the HEH_2 concentration throughout the experiments. Titrations were done under a sparging N_2 atmosphere to maintain an O_2 free environment. Experiments were conducted at 23 °C.

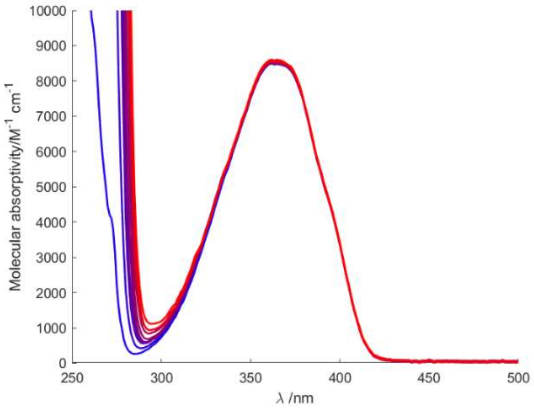

Figure C.11. UV-vis of HEH_2 (0.1 mM) with 0 mM (blue) to 14 mM (red) Col concentration.

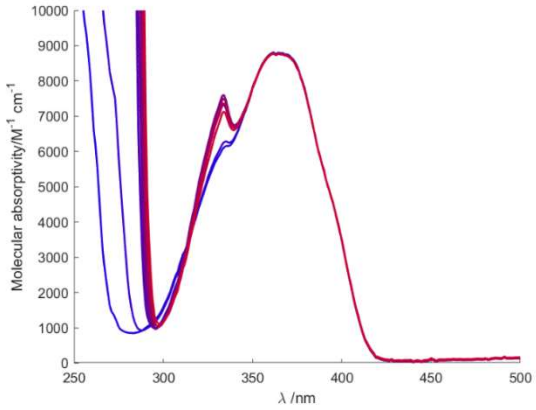

Figure C.12. UV-vis of HEH_2 (0.1 mM) with 0 mM (blue) to 11 mM (red) [ColH]OTf concentration.

C.5 Reduction of $[TBA]NO_3$

Proposed balanced equation:

$$[TBA]NO_3 + 4\,HEH_2 + [ColH]OTf \longrightarrow NH_3 + 4\,HE + 3\,H_2O + Col + [TBA]OTf$$

Scheme C.1. Balanced equation for the catalytic reduction of $[TBA]NO_3$ to generate NH_3.

C.5.1 Standard $[TBA]NO_3$ Reduction Generation Reaction Procedure

Catalytic experiments for the reduction of $[TBA]NO_3$ were conducted in a manner similar to the reduction of N_2 (section **S1.1**). All solvents are stirred with Na/K for ≥2 hours and filtered prior to use. In a nitrogen-filled glovebox, the precatalysts ($[MoBr_3]$ and $[Ir]BAr^F{}_4$) (2.3 μmol) are weighed in individual vials.* The precatalysts are then transferred quantitatively into a Schlenk tube using THF. The THF is then evaporated to provide a thin film of precatalyst at the bottom of the Schlenk tube. The tube is then charged with a stir bar, and the [TBA]NO3, acid, and Hantzsch ester (HEH 2) are added as solids. The tube is cooled to 77 K in a cold well, and the base ([Col]) is added. The tubes were passed out of the glovebox without warming and thoroughly degassed. 1 mL of degassed (three freeze-pump thaw cycles) THF solvent was vacuum transferred into the catalytic tube. The tube was allowed to warm briefly and was backfilled with argon. The tube is instead transferred to a

water bath, where it thaws and is allowed to stir for 12 hours. To ensure reproducibility, all experiments were conducted in 200 mL Schlenk tubes (50 mm OD) using 10 mm egg-shaped stir bars, and stirring was conducted at ~600 rpm. The water bath was contained in highly reflective dewars. The Blue LED was placed above the bath as close to the stirring reaction as possible.

C.5.2 NH_3 detection

NH_3 was detected by ^1H NMR, as detailed in C.2.4 NH_3 detection by ^1H NMR.

C.5.3 Catalytic reduction of [TBA]$^{15}NO_3$

Catalytic runs were set-up as described in **S5.1** but using [TBA]$^{15}NO_3$.

C.5.4 Catalytic reduction of [TBA]NO_3

Table C.7. Catalytic yields for photodriven transfer hydrogenation of [TBA]NO_3 to NH_3

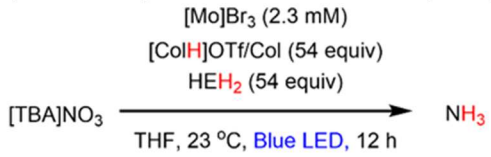

Run	Conditions	[$MoBr_3$] load (μmol)	acid (μmol)	base (μmol)	Ir (μmol)	HEH_2 /Mo	[TBA] NO_3 equiv/Mo	NH_3 equiv /Mo	NH_3 yield/ HEH_2 (%)
Table 4.1, entry 27: Standard conditions for reduction of [TBA]NO_3									
A7	THF, 23 °C	2.3	124.2	124.2	**0**	54	18	8.5	
B7	THF, 23 °C	2.3	124.2	124.2	**0**	54	18	11.0	
	THF, 23 °C	2.3	124.2	124.2	0	54	18	9.8±1.2	73±9
Table 4.1, entry 28: with [$MoBr_3$] , with [Ir]$BAr^F{}_4$									
C7	THF, 23 °C	2.3	124.2	124.2	**2.3**	54	18	9.9	
D7	THF, 23 °C	2.3	124.2	124.2	**2.3**	54	18	10.9	
	THF, 23 °C	2.3	124.2	124.2	**2.3**	54	18	10.4±0.5	77±4
Table 4.1, entry 29: No [$MoBr_3$]									
E7	THF, 23 °C	2.3	124.2	124.2	**2.3**	54	18	2	
F7	THF, 23 °C	2.3	124.2	124.2	**2.3**	54	18	1.4	
	THF, 23 °C	2.3	124.2	124.2	**2.3**	54	18	1.7±0.3	13±2
Table 4.1, entry 30: No [$MoBr_3$] , with [Ir]$BAr^F{}_4$									
F7	THF, 23 °C	2.3	124.2	124.2	**2.3**	54	18	3.0	
G7	THF, 23 °C	2.3	124.2	124.2	**2.3**	54	18	5.4	
	THF, 23 °C	2.3	124.2	124.2	**2.3**	54	18	4.2±1.2	31±9

Table 4.1, entry 31: no light, with [$MoBr_3$] , with [Ir]BAr^F_4

H7	THF, 23 °C No light	2.3	124.2	124.2	**2.3**	54	18	0.1	
I7	THF, 23 °C No light	2.3	124.2	124.2	**2.3**	54	18	0.1	
	THF, 23 °C No light	2.3	124.2	124.2	**2.3**	54	18	0.1±0.05	0.7±0.3

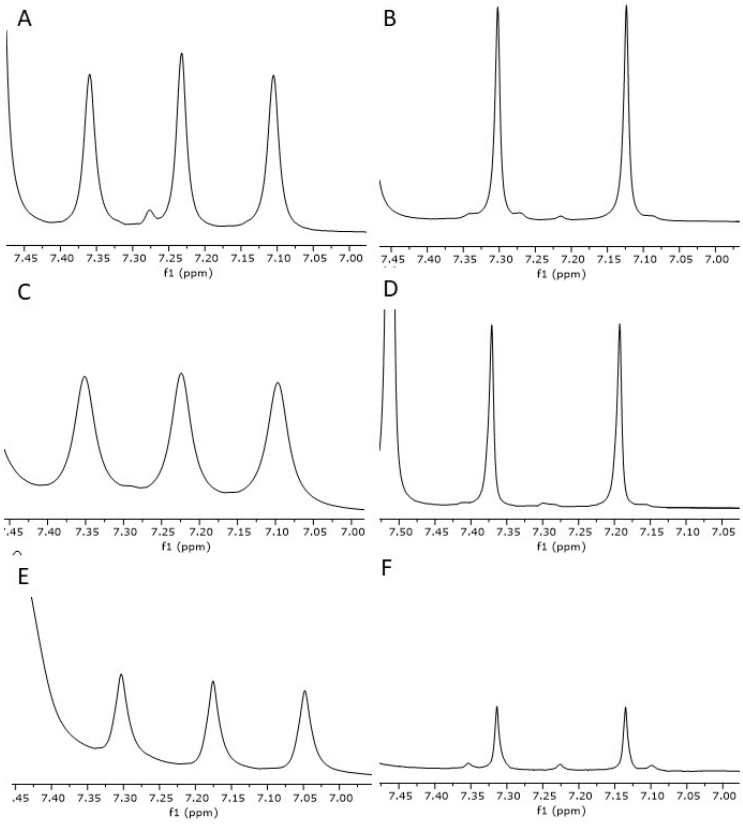

Figure C.13. ^{1}H NMR (DMSO-d_6, 400 MHz) of: A) $^{14}NH_4Cl$ obtained from reaction of natural abundance [TBA]NO_3 with HEH_2, buffer, and [$MoBr_3$] under blue light irradiation (Table C.7 entry A7); B) $^{15}NH_4Cl$ obtained from reaction of [TBA]$^{15}NO_3$ with HEH_2, buffer, and [$MoBr_3$] under blue light irradiation; C) $^{14}NH_4Cl$ obtained from reaction of natural abundance [TBA]NO_3 with HEH_2, buffer, [$MoBr_3$] and [Ir]BAr^F_4 under blue light irradiation (Table C.7, entry C7); D) $^{15}NH_4Cl$ obtained from reaction of [TBA]$^{15}NO_3$ with HEH_2, buffer, [$MoBr_3$] and [Ir]BAr^F_4 under blue light irradiation; E) $^{14}NH_4Cl$ obtained from reaction of natural abundance [TBA]NO_3 with HEH_2, buffer, and [Ir]BAr^F_4 under blue light irradiation (Table C.7, entry F7); F) $^{15}NH_4Cl$ obtained from reaction of [TBA]$^{15}NO_3$ with HEH_2, buffer, and [Ir]BAr^F_4 under blue light irradiation.

C.5.5 Comment on nitrate reduction in the absence of light or [$MoBr_3$].

It is worth commenting on the fact that [TBA]NO_3 reduction can occur both in the absence of light and [$MoBr_3$], albeit with diminished yields. This differs from N_2R where both are required and no NH_3 can be detected. Nitrate differs as a substrate from N_2 in that it is more activated and forms relatively stable intermediates during reduction (NO_2^-, NO), and the thermodynamics of reduction are more favorable. This is illustrated in Figure C.14, showing the thermodynamics between different intermediates in the reduction of N2 and NO_3^- (in aqueous solution vs NHE). Therefore, a molecular catalyst might not be required to activate the substrate prior to reduction/protonation and stabilize intermediates that form during reduction. The role of [$MoBr_3$] might, therefore, be primarily as a Lewis acid or a solubilizing agent. Ultimately, these results suggest that higher yields/efficiencies and possibly even nitrate reduction without illumination may all be possible with a more careful choice of catalyst and warrant further exploration.

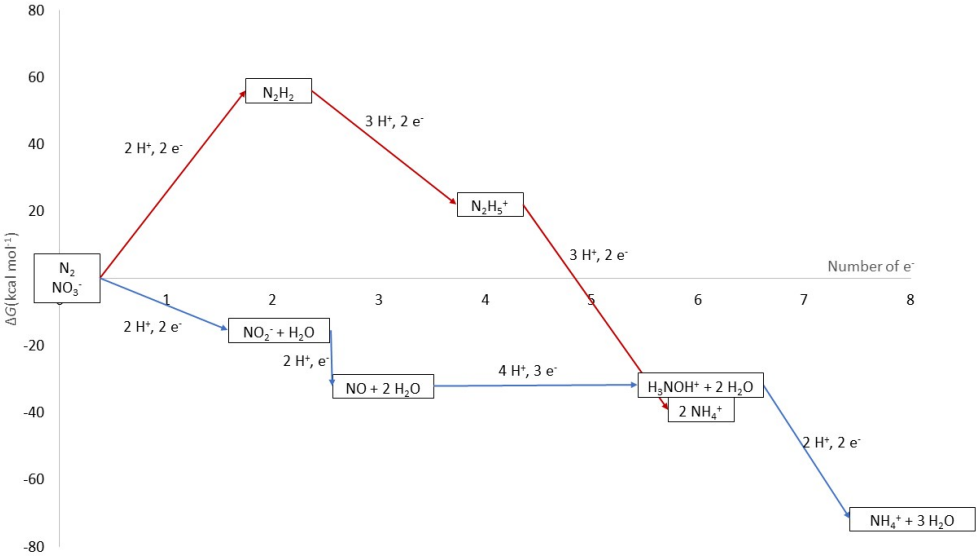

Figure C.14. Comparison of ΔG (in kcal mol^{-1}) in aqueous solution of pH 0 referenced to NHE.[13,14] While the 6 e^- reduction and 8 e^- reduction of N_2 and NO_3^-, respectively, are both downhill, only the intermediates of NO_3^- are also thermodynamically favored to form.

C.6 Reduction of acetylene

Proposed balanced equations:

$$C_2H_2 + HEH_2 \longrightarrow C_2H_4 + HE$$

$$C_2H_4 + HEH_2 \longrightarrow C_2H_6 + HE$$

Scheme C.2. Balanced equations for the catalytic reduction of acetylene to generate ethylene and ethane.

C.6.1 Standard acetylene reduction reaction procedure

Catalytic experiments for the reduction of acetylene were conducted in a manner similar to the reduction of N_2 (section **S1.1**). All solvents are stirred with Na/K for ≥2 hours and filtered prior to use. In a nitrogen-filled glovebox, the precatalysts ([$MoBr_3$] and [Ir]BAr^F_4) (2.5 μmol) are weighed in individual vials. The precatalysts are then transferred quantitatively into a Schlenk tube using THF. The THF is then evaporated to provide a thin film of precatalyst at the bottom of the Schlenk tube. The tube is then charged with a stirbar and [ColH]OTf and Hantzsch ester (HEH_2) are added to the vial as solids. The tube is wrapped in aluminum foil and Col and THF-d_8 (0.7 mL) are added. The tube is sealed, passed out of the glovebox, and degassed (three freeze-pump thaw cycles). The desired volume of acetylene gas is added using a calibrated bulb while the tube is cooled in liquid nitrogen. The headspace of the tube is then backfilled to 1 atm with argon while cooled in a dry ice/acetone bath. The tube is transferred to a water bath and is irradiated with Blue LED for the time specified. The water bath was contained in highly reflective dewars. The Blue LED was placed above the bath as close to the reaction as possible.

After 12 hours of irradiation, the volatiles of the reaction mixture are vacuum transferred into a J. Young NMR tube of known volume containing a known amount of 1,3,5-trimethoxybenzene. In the ^{1}H NMR spectrum of the resulting sample, the peaks corresponding to ethylene (5.36 ppm) and ethane (0.85 ppm) are distinguishable when present.[10] Integration to the internal standard provides the yield of dissolved gases. Henry's constant for each gas in THF[15] was used to estimate their partial pressures in the headspace.

C.6.2 Ethylene and ethane detection results

Table C.8. Catalytic yields for photodriven transfer hydrogenation of acetylene to ethylene and ethane.

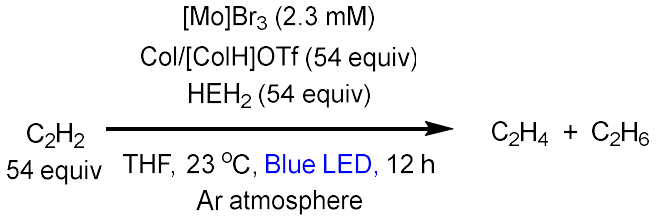

Run	Conditions	[Mo] load (μmol)	acid (μmol)	base (μmol)	Ir (μmol)	HEH_2 equiv /Mo	C_2H_4 equiv /Mo	C_2H_6 equiv/ Mo	Total yield/ HEH_2 (%)
Table 4.1, entry 32: standard conditions									
A8	THF, 23 °C	2.5	135	135	0	54	8.2	1.3	
B8	THF, 23 °C	2.5	135	135	0	54	11.4	1.7	
	THF, 23 °C	2.5	135	135	0	54	10±2	1.5±0.3	24±5
Table 4.1, entry 33: with [$MoBr_3$], with [Ir]BAr^F_4									
C8	THF, 23 °C	2.5	135	135	2.5	54	6.4	1.3	
D8	THF, 23 °C	2.5	135	135	2.5	54	4.9	0.9	
	THF, 23 °C	2.5	135	135	2.5	54	6±1	1.1±0.3	15±3
Table 4.1, entry 34: no [$MoBr_3$], no [Ir]BAr^F_4									
E8	THF, 23 °C	2.5	135	135	0	54	0.048	<0.03	
F8	THF, 23 °C	2.5	135	135	0	54	0.059	<0.03	
	THF, 23 °C	2.5	135	135	0	54	0.054± 0.008	<0.03	<0.3
Table 4.1, entry 35: no [$MoBr_3$], with [Ir]BAr^F_4									
G8	THF, 23 °C	0	135	135	2.5	54	0.8	0.02	
H8	THF, 23 °C	0	135	135	2.5	54	3.0	0.14	
	THF, 23 °C	0	135	135	2.5	54	2±2	0.08± 0.08	4±3
Table 4.1, entry 36: with [$MoBr_3$], with [Ir]BAr^F_4, no light									
I8	THF, 23 °C no light	2.5	135	135	2.5	54	<0.01	<0.01	
J8	THF, 23 °C no light	2.5	135	135	2.5	54	<0.01	<0.01	
	THF, 23 °C no light	2.5	135	135	2.5	54	<0.01	<0.01	<0.04

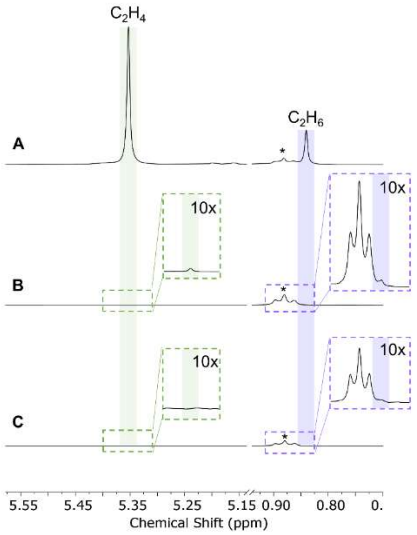

Figure C.15. ^{1}H NMR (THF-d_8, 400 MHz) of the volatiles obtained from the acetylene reduction reaction in Table C.8: A) Standard conditions (Table C.8, entry A8); B) No [$MoBr_3$] (Table C.8, entry E8); C) No irradiation (Table C.8, entry I8). *Trace pentane.

C.7. Additional mechanistic schemes

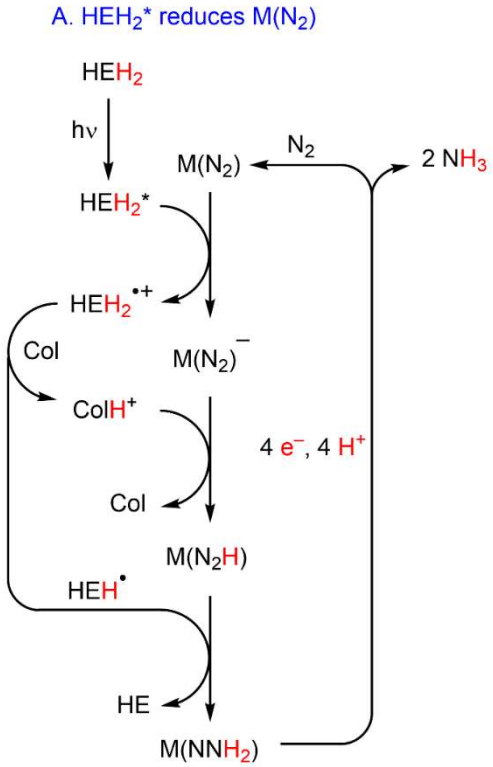

Figure C.16. Mechanistic scenario in absence of photoredox catalyst in which $[HEH_2]^*$ is quenched by a $M(N_2)$ intermediate.

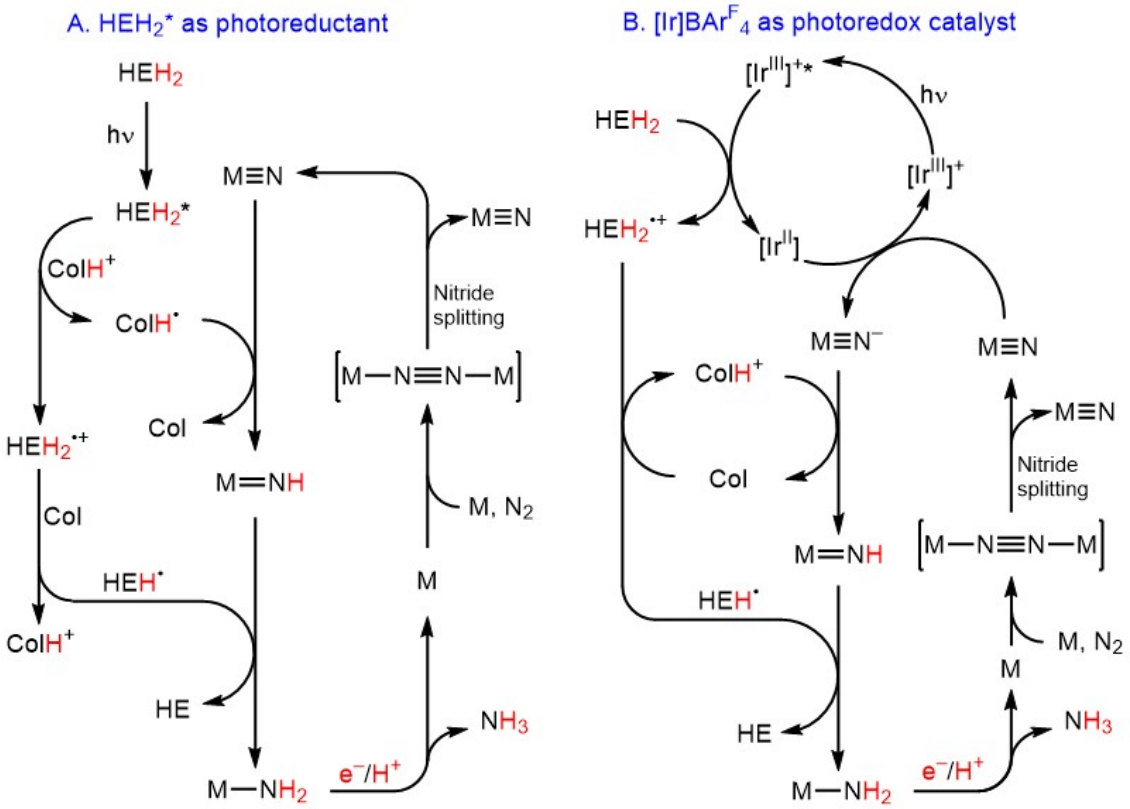

Figure C.17. Possible scenarios for photodriven transfer hydrogenation from HEH_2 to N_2 mediated by a metal catalyst and buffer system (Col/$[ColH]^+$). These schemes depict a mechanism in which N_2 cleavage occurs and the subsequent M≡N is hydrogenated. (A) Scenario in the absence of photoredox catalyst, in which $[HEH_2]$* is oxidatively quenched by $[ColH]^+$ to generate $[ColH]^•$. (B) Scenario with photoredox catalyst, in which $[Ir^{III}]^+$* is reductively quenched by HEH_2.

C.8 Derivation of thermodynamic values.

C.8.1 Summary of thermochemistry of Hantzsch ester (HEH_2) and derivatives

Table C.9 lists $BDFE_{X–H}$, pK_a, and E_{ox} values for various protonation and oxidation states of HEH_2. As has been established by Mayer and coworkers,[16] bond dissociation enthalpies (BDEs) can be converted to BDFEs based on the assumption that the entropies of R–H and R$^•$ are similar. Subtraction of $TS°(H^•)_{solv}$ (6.37 kcal mol^{-1} in MeCN) from the BDE values reported in ref. 4 yields the estimated BDFE values in Table C.9. With these values and reported potentials of oxidation, relevant pK_a values were then estimated using the thermodynamic cycles laid out below.

Table C.9. Reported and estimated thermochemical values for various protonation and oxidation states of HEH_2 relevant to this study. [a] kcal mol^{-1} in MeCN at 298 K. [b] V vs. $Fc^{+/0}$ in MeCN at 298 K. [c] Ref. 4. [d] Estimated using the E_{00} reported in ref. 17.

	BDE[a]	BDFE[a]	E_{ox}[b]	pK_a
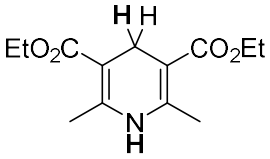 HEH_2	68.7 (C–H), 86.6 (N–H)[c]	62.3 (C–H), 80.2 (N–H)	0.48[c]	31.8 (N–H)
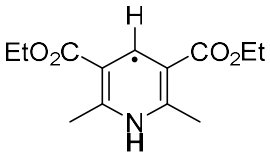 $HEH^{\bullet}$	46.9 (N–H)[c]	40.5 (N–H)		
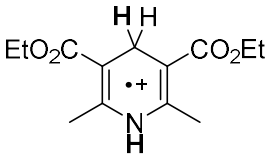 $HEH^{\bullet+}$				–1.0 (C–H)
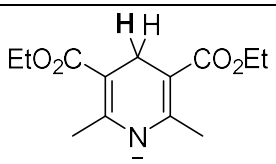 HEH^{-}			–0.695[c]	
$[HEH_2]$*		–8.5 (C–H)[d]	–2.5[d]	–20(N–H)[d]

Estimation of the N–H pK_a of HEH_2:

$HEH^{\bullet} + e^{-} \rightleftharpoons HEH^{-}$ $\quad -23.06(E_{ox}(HEH^{-})) = 16$ kcal mol^{-1}
$H^{\bullet} \rightleftharpoons H^{+} + e^{-}$ $\quad -C_G = -52.6$ kcal mol^{-1}
$\underline{HEH_2 \rightleftharpoons HEH^{\bullet} + H^{\bullet}\ \ BDFE_{N-H}(HEH_2) = 80.2 \text{ kcal mol}^{-1}}$
$HEH_2 \rightleftharpoons HEH^{-} + H^{+}$ $\quad 1.37(pK_a)$
$pK_{a,N-H}(HEH_2) = \mathbf{31.8}$

Estimation of the C–H pK_a of $HEH_2^{\bullet+}$:

$HEH_2^{\bullet} + e^{-} \rightleftharpoons HEH_2$ $\quad -23.06(E_{ox}(HEH_2)) = -11.1$ kcal mol^{-1}
$H^{\bullet} \rightleftharpoons H^{+} + e^{-}$ $\quad -C_G = -52.6$ kcal mol^{-1}
$\underline{HEH_2 \rightleftharpoons HEH^{\bullet} + H^{\bullet}\ \ BDFE_{C-H}(HEH_2) = 62.3 \text{ kcal mol}^{-1}}$
$HEH_2^{\bullet+} \rightleftharpoons HEH^{\bullet} + H^{+}$ $\quad 1.37(pK_a)$
$pK_{a,C-H}(HEH^{\bullet+}) = \mathbf{-1.0}$

Estimation of the excited-state N–H pK_a of [HEH_2]*:

$HEH_2^* \rightleftharpoons HEH_2$ $-23.06(E_{00}) = -70.8$ kcal mol^{-1}
$\underline{HEH_2 \rightleftharpoons HEH^- + H^+ \quad 1.37(pK_{a,N-H}(HEH_2)) = 43.6 \text{ kcal mol}^{-1}}$
$HEH_2^* \rightleftharpoons HEH^- + H^+ \quad 1.37(pK_a)$
$pK_{a,N-H}(HEH_2^*) = \mathbf{-20}$

Estimation of the excited-state $BDFE_{C-H}$ of [HEH_2]*:

$HEH_2^* \rightleftharpoons HEH_2$ $-23.06(E_{00}) = -70.8$ kcal mol^{-1}
$\underline{HEH_2 \rightleftharpoons HEH^- + H^+ \quad BDFE_{C-H}(HEH_2) = 62.3 \text{ kcal mol}^{-1}}$
$HEH_2^* \rightleftharpoons HEH^- + H^+ \quad BDFE_{C-H}(HEH_2^*) = \mathbf{-8.5 \text{ kcal mol}^{-1}}$

C.8.2 Derivation of effective BDFE values ($BDFE_{eff}$) relevant to this work

C.8.2.1 Derivation of $BDFE_{eff}$ for H_2-carrier

Estimation of $BDFE_{eff}$ for HEH_2:

½ $HEH_2 \rightleftharpoons$ ½ $HEH^\bullet$ + ½ $H^\bullet$ ½ $BDFE_{C-H}(HEH_2) = 31.2$ kcal mol^{-1}
$\underline{\text{½ } HEH^\bullet \rightleftharpoons \text{½ HE} + \text{½ } H^\bullet \text{ ½ } BDFE_{N-H}(HEH^\bullet) = 20.3 \text{ kcal mol}^{-1}}$
½ $HEH_2 \rightleftharpoons$ ½ HE + $H^\bullet$ $BDFE_{eff}(HEH_2) = \mathbf{51.4 \text{ kcal mol}^{-1}}$

Estimation of $BDFE_{eff}$ for $acrH_2$:

$acrH_2 \rightleftharpoons acrH_2^{\bullet+} + e^-$ $23.06(E_{ox}(acrH_2)) = 11.3$ kcal mol^{-1} (Ref 18)
$acrH_2^{\bullet+} \rightleftharpoons acrH^+ + H^\bullet$ $BDE(acrH_2^{\bullet+}) - TS°(H^\bullet)_{solv} = 43.5 - 6.37$ kcal mol^{-1} $= 37.1$ kcal mol^{-1} (Ref 51)
$\underline{e^- + H^\bullet \rightleftharpoons H^- \quad \Delta G° = 26.0 \text{ kcal mol}^{-1} \text{ (Ref 16)}}$
$acrH_2 \rightleftharpoons acrH^+ + \underline{H^-}$ $\Delta G(acrH_2)_{H^-} = \mathbf{74.4 \text{ kcal mol}^{-1}}$

½ $acrH_2 \rightleftharpoons$ ½ $acrH^+$ + ½ H^- ½ $\Delta G(acrH_2)_{H^-} = 37.2$ kcal mol^{-1}
½ $acrH^+ \rightleftharpoons$ ½ acr + ½ H^+ ½ $1.37(\underline{pK_a}) = 8.7$ kcal mol^{-1} (Ref 19)
½ H^- + ½ $H^+ \rightleftharpoons$ ½ H_2 ½ $\Delta G° = -38$ kcal mol^{-1} (Ref 16)
$\underline{\text{½ } H_2 \rightleftharpoons H^\bullet \quad \text{½ } BDFE_{N-H}(H_2) = 52 \text{ kcal mol}^{-1}}$
½ BNAH + $\underline{\text{½}}$ $[ColH]^+ \rightleftharpoons$ ½ BNA + ½ Col + $H^\bullet$ $BDFE_{eff}(acrH_2) = \mathbf{59.9 \text{ kcal mol}^{-1}}$

Estimation of $BDFE_{eff}$ for $phenH_2$:

½ $phenH_2 \rightleftharpoons$ ½ $phenH^\bullet$ + ½ $H^\bullet$ ½ $BDFE_{C-H}(phenH_2) = 33.1$ kcal mol^{-1} (Ref 4)
$\underline{\text{½ } phenH^\bullet \rightleftharpoons \text{½ phen} + \text{½ } H^\bullet \text{½ } BDFE_{N-H}(phenH^\bullet) = 19.1 \text{ kcal mol}^{-1} \text{ (Ref 4)}}$
½ $phenH_2 \rightleftharpoons$ ½ phen + $H^\bullet$ $BDFE_{eff}(phenH_2) = \mathbf{52.2 \text{ kcal mol}^{-1}}$

Estimation of $BDFE_{eff}$ for BNAH:

BNAH is a 1 H^+ /2 e^- donor. As such, to balance the equation for the 6 H^+/6 e^- reduction of N_2, we posit that [ColH]OTf must also be consumed giving a balanced reaction:
$N_2 + 3\ BNAH + 3\ [ColH]^+ \rightarrow NH_3 + 3\ [BNA]^+ + 3\ Col$
To estimate $BDFE_{eff}$, we instead combine the hydricity of BNAH and the acidity of [ColH]OTf

½ BNAH ⇌ ½ BNA + ½ H^- ½ $\Delta G(BNAH)_{H^-}$ = 29.5 kcal mol^{-1} (Ref 18)
½ $[ColH]^+$ ⇌ ½ Col + ½ H^+ ½ 1.37(pK_a) = 10.3 kcal mol^{-1} (Ref 20)
½ H^- + ½ H^+ ⇌ ½ H_2 ½ $\Delta G°$ = −38 kcal mol^{-1} (Ref 16)
½ H_2 ⇌ $H^•$ ½ $BDFE_{N–H}(H_2)$ = 52 kcal mol^{-1}
½ BNAH + ½ $[ColH]^+$ ⇌ ½ BNA + ½ Col + $H^•$ $BDFE_{eff}(BNAH/ColH^+)$ = **53.8 kcal mol^{-1}**

C.8.2.2 Derivation of $BDFE_{eff}$ for reductant (photosensitizer or *HEH_2) and acid

Estimation of $BDFE_{eff}$ for $[HEH_2]$* as reductant and $[ColH]^+$ as acid:

$HEH_2^* \rightleftharpoons HEH_2^{•+} + e^-$ 23.06(E_{ox}([*HEH_2]) = –57.7 kcal mol^{-1}
$[ColH]^+ \rightleftharpoons Col + H^+$ 1.37(pK_a) = 20.6 kcal mol^{-1}
$H^+ + e^- \rightleftharpoons H^•$ C_G = 52.6 kcal mol^{-1}
$HEH_2^* + [ColH]^+ \rightleftharpoons HEH_2^{•+} + Col + H^•$ $BDFE_{eff}$ = **15.5 kcal mol^{-1}**

Estimation of $BDFE_{eff}$ for $Ir^{II}(ppy)_2$(dtbbpy) as reductant and $[ColH]^+$ as acid:

$[Ir^{II}] \rightleftharpoons [Ir^{III}]^+ + e^-$ 23.06(E_{ox}([Ir^{II}]) = –43.8 kcal mol^{-1} (Ref 21)
$[ColH]^+ \rightleftharpoons Col + H^+$ 1.37(pK_a) = 20.6 kcal mol^{-1}
$H^+ + e^- \rightleftharpoons H^•$ C_G = 52.6 kcal mol^{-1}
$HEH_2^* + [ColH]^+ \rightleftharpoons HEH_2^{•+} + Col + H^•$ $BDFE_{eff}$ = **29.3 kcal mol^{-1}**

Estimation of $BDFE_{eff}$ for Ir^{II}(*p*-F(Me)ppy)$_2$(dtbbpy) as reductant and $[ColH]^+$ as acid:

$[Ir^{II}] \rightleftharpoons [Ir^{III}]^+ + e^-$ 23.06(E_{ox}([Ir^{II}]) = –43.4 kcal mol^{-1} (Ref 22)
$[ColH]^+ \rightleftharpoons Col + H^+$ 1.37(pK_a) = 20.6 kcal mol^{-1}
$H^+ + e^- \rightleftharpoons H^•$ C_G = 52.6 kcal mol^{-1}
$HEH_2^* + [ColH]^+ \rightleftharpoons HEH_2^{•+} + Col + H^•$ $BDFE_{eff}$ = **29.8 kcal mol^{-1}**

Estimation of $BDFE_{eff}$ for $Ir^{II}(dF(CF_3)ppy)_2$(dtbbpy) as reductant and $[ColH]^+$ as acid:

$[Ir^{II}] \rightleftharpoons [Ir^{III}]^+ + e^-$ 23.06(E_{ox}([Ir^{II}]) = –40.4 kcal mol^{-1} (Ref 23)
$[ColH]^+ \rightleftharpoons Col + H^+$ 1.37(pK_a) = 20.6 kcal mol^{-1}
$H^+ + e^- \rightleftharpoons H^•$ C_G = 52.6 kcal mol^{-1}
$HEH_2^* + [ColH]^+ \rightleftharpoons HEH_2^{•+} + Col + H^•$ $BDFE_{eff}$ = **32.8 kcal mol^{-1}**

Estimation of $BDFE_{eff}$ for $[Ir^{II}(ppy)_3]^-$ as reductant and $[ColH]^+$ as acid:

$[Ir^{II}] \rightleftharpoons [Ir^{III}]^+ + e^-$ $23.06(E_{ox}([Ir^{II}]) = -59.3$ kcal mol^{-1} (Ref 23)
$[ColH]^+ \rightleftharpoons Col + H^+$ $1.37(pK_a) = 20.6$ kcal mol^{-1}
$H^+ + e^- \rightleftharpoons H^\bullet$ $C_G = 52.6$ kcal mol^{-1}
$HEH_2^* + [ColH]^+ \rightleftharpoons HEH_2^{\bullet+} + Col + H^\bullet$ $BDFE_{eff}$ = **13.9 kcal mol^{-1}**

Estimation of $BDFE_{eff}$ for $[Ir^{III}(ppy)_3]^*$ as reductant and $[ColH]^+$ as acid:

$[Ir^{II}] \rightleftharpoons [Ir^{III}]^+ + e^-$ $23.06(E_{ox}([Ir^{III*}]) = -48.7$ kcal mol^{-1} (Ref 23)
$[ColH]^+ \rightleftharpoons Col + H^+$ $1.37(pK_a) = 20.6$ kcal mol^{-1}
$H^+ + e^- \rightleftharpoons H^\bullet$ $C_G = 52.6$ kcal mol^{-1}
$HEH_2^* + [ColH]^+ \rightleftharpoons HEH_2^{\bullet+} + Col + H^\bullet$ $BDFE_{eff}$ = **24.5 kcal mol^{-1}**

C.8.3 Estimation of overpotential for hydrogenation of N_2 with HEH_2 to NH_3

We derive the BDFE of H_2 in MeCN at 298 K explicitly here for clarity, using recently updated thermochemical values (*36*):

$H_{2(g)} \rightleftharpoons 2\ H^+ + 2\ e^-$ $2\times23.06(E°(H^+/H_2)) = 2\times23.06(-0.028\ V) = -1.29$ kcal mol^{-1} (Ref 16)
$2\ H^+ + 2\ e^- \rightleftharpoons 2H^\bullet$ $2(C_G) = 105.2$ kcal mol^{-1}
$H_{2(g)} \rightleftharpoons 2H^\bullet$ $BDFE(H_2)$ = **103.9 kcal mol^{-1}**

C.8.3.1 Determination of overpotential for dark reactions

The overpotential $\Delta\Delta G_f(NH_3)$ for a source of hydrogen atom equivalents with a given $BDFE_{eff}$ is described by eqn C.3:

$$\Delta\Delta G_f(NH_3) = 3(BDFE(H_2)/2 - BDFE_{eff}) \text{ (eqn C.3)}$$

For the dark reaction, $\frac{1}{2}\ N_2 + \frac{3}{2}\ HEH_2 \rightleftharpoons NH_3 + \frac{3}{2}\ HE$:

$$\Delta\Delta G_f(NH_3) = 3(103.9/2 - 51.4) = \textbf{1.7 kcal mol}^{-1}$$

For the dark reaction, $\frac{1}{2}\ N_2 + \frac{3}{2}\ acrH_2 \rightleftharpoons NH_3 + \frac{3}{2}$ acr:

$$\Delta\Delta G_f(NH_3) = 3(103.9/2 - 59.9) = \textbf{-23.9 kcal mol}^{-1}$$

For the dark reaction, $\frac{1}{2}\ N_2 + \frac{3}{2}\ phenH_2 \rightleftharpoons NH_3 + \frac{3}{2}$ phen:

$$\Delta\Delta G_f(NH_3) = 3(103.9/2 - 52.2) = \textbf{-0.8 kcal mol}^{-1}$$

For the dark reaction, $\frac{1}{2}\ N_2 + \frac{3}{2}\ (BNAH + ColH^+) \rightleftharpoons NH_3 + \frac{3}{2}\ (BNA^+ + Col)$:

$$\Delta\Delta G_f(NH_3) = 3(103.9/2 - 53.8) = \textbf{-5.5 kcal mol}^{-1}$$

With the dark reaction values value, we can also estimate the absolute driving force for hydrogenation of N_2 with $subH_2$.

$\Delta G_f(NH_3)$ in MeCN at 298 K:

$^1/_2$ N_2 + $^3/_2$ $H_{2(g)}$ ⇌ NH_3 $\Delta G_f(NH_3) = -3\times23.06(E°(N_{2(g)}/NH_3)) = -3\times23.06(0.063$ V vs. $H_2)$ (Ref 36)

$$= \mathbf{4.36\ kcal\ mol^{-1}}$$

We then estimate the following:

$^1/_2$ N_2 + $^3/_2$ HEH_2 ⇌ NH_3 + $^3/_2$ HE$\Delta G_{rxn} = \Delta G_f(NH_3) - \Delta\Delta G_f(NH_3, HEH_2) = -4.4 - 1.7$ kcal mol^{-1}

$$= \mathbf{-6.1\ kcal\ mol^{-1}}$$

$^1/_2$ N_2 + $^3/_2$ $phenH_2$ ⇌ NH_3 + $^3/_2$ phen $\Delta G_{rxn} = \Delta G_f(NH_3) - \Delta\Delta G_f(NH_3, phenH_2) = -4.4 + 0.8$ kcal mol^{-1}

$$= \mathbf{-3.6\ kcal\ mol^{-1}}$$

$^1/_2$ N_2 + $^3/_2$ $acrH_2$ ⇌ NH_3 + $^3/_2$ acr $\Delta G_{rxn} = \Delta G_f(NH_3) - \Delta\Delta G_f(NH_3, acrH_2) = -4.4 + 23.9$ kcal mol^{-1}

$$= \mathbf{19.5\ kcal\ mol^{-1}}$$

$^1/_2$ N_2 + $^3/_2$ (BNAH + $ColH^+$) ⇌ NH_3 + $^3/_2$ (BNA^+ + Col)

$\Delta G_{rxn} = \Delta G_f(NH_3) - \Delta\Delta G_f(NH_3, BNAH + ColH^+) = -4.4 + 5.5$ kcal mol^{-1}

$$= \mathbf{+1.1\ kcal\ mol^{-1}}$$

Table C.10. Summary of driving forces for dark reaction using different $subH_2$ (assuming 2 H^+/ 2 e^- reaction). Values are calculated in MeCN at 25 °C. [a] Since BNAH is a H^- donor, the stoichiometry requires addition of H^+, assumed to be supplied from [ColH]OTf

$subH_2$	$BDFE_{eff}$ (kcal mol^{-1})	$\Delta\Delta G_f(NH_3)$ (kcal mol^{-1})	ΔG_{rxn} (kcal mol^{-1})
HEH_2	51.4	1.7	−6.1
$PhenH_2$	52.2	−0.8	−3.6
$AcrH_2$	59.9	−23.9	19.5
BNAH + [ColH]OTf [a]	53.8	−5.5	1.1

C.8.3.2 Determination of overpotential for light reactions

For the Ir-free reaction, in which $[HEH_2]$* is thought to be the strongest reductant accessed and $[ColH]^+$ serves as acid:

$$\Delta\Delta G_f(NH_3) = 3(103.9/2 - 15.5) = \mathbf{109\ kcal\ mol^{-1}}$$

For the Ir-photosensitized reaction with $[Ir(ppy)_2(dtbbpy)]BAr^F{}_4$, in which $[Ir^{II}]$ is thought to be the strongest reductant accessed and $[ColH]^+$ serves as acid:

$$\Delta\Delta G_f(NH_3) = 3(103.9/2 - 29.3) = \mathbf{68.0\ kcal\ mol^{-1}}$$

For the Ir-photosensitized reaction with $[Ir(dF(CF_3)ppy)_2(dtbbpy)]PF_6$, in which $[Ir^{II}]$ is thought to be the strongest reductant accessed and $[ColH]^+$ serves as acid:

$$\Delta\Delta G_f(NH_3) = 3(103.9/2 - 32.8) = \mathbf{58.3\ kcal\ mol^{-1}}$$

For the Ir-photosensitized reaction with $[Ir(p\text{-}F(Me)ppy)_2(dtbbpy)]PF_6$, in which $[Ir^{II}]$ is thought to be the strongest reductant accessed and $[ColH]^+$ serves as acid:

$$\Delta\Delta G_f(NH_3) = 3(103.9/2 - 29.8) = \mathbf{67.3\ kcal\ mol^{-1}}$$

For the Ir-photosensitized reaction with $Ir(ppy)_3$, in which $[Ir^{II}]$ is thought to be the strongest reductant accessed and $[ColH]^+$ serves as acid:

$$\Delta\Delta G_f(NH_3) = 3(103.9/2 - 13.9) = \mathbf{115.0\ kcal\ mol^{-1}}$$

For the Ir-photosensitized reaction with $Ir(ppy)_3$, in which $[Ir^{III}]$* is thought to be the strongest reductant accessed and $[ColH]^+$ serves as acid:

$$\Delta\Delta G_f(NH_3) = 3(103.9/2 - 24.5) = \mathbf{83.2\ kcal\ mol^{-1}}$$

Table C.11: Summary of driving forces for different photosensitizers. All $BDFE_{eff}$ and $\Delta\Delta G_f(NH_3)$ measurements made pairing reductant with [ColH]OTf (pK_a 15) Values are calculated in MeCN at 25 °C.

Reductant	E_{ox} (V vs. $Fc^{+/0}$)	$BDFE_{eff}$ (kcal mol^{-1})	$\Delta\Delta G_f(NH_3)$ (kcal mol^{-1})
HEH_2*	−2.5	15.5	109
$[Ir^{II}]$ ($Ir^{II}(ppy)_2dtbbpy$)	−1.90	29.3	68.0
$Ir^{II}(dF(CF_3)ppy)_2(dtbbpy)$	−1.75	32.8	58.3
Ir^{II}(*p*-F(Me)ppy)$_2$(dtbbpy)	−1.88	29.8	67.3
$Ir^{II}(ppy)_3^-$	−2.57	13.9	115.0
$Ir^{III}(ppy)_3$*	−2.11	24.5	83.2

C.9 NMR spectra

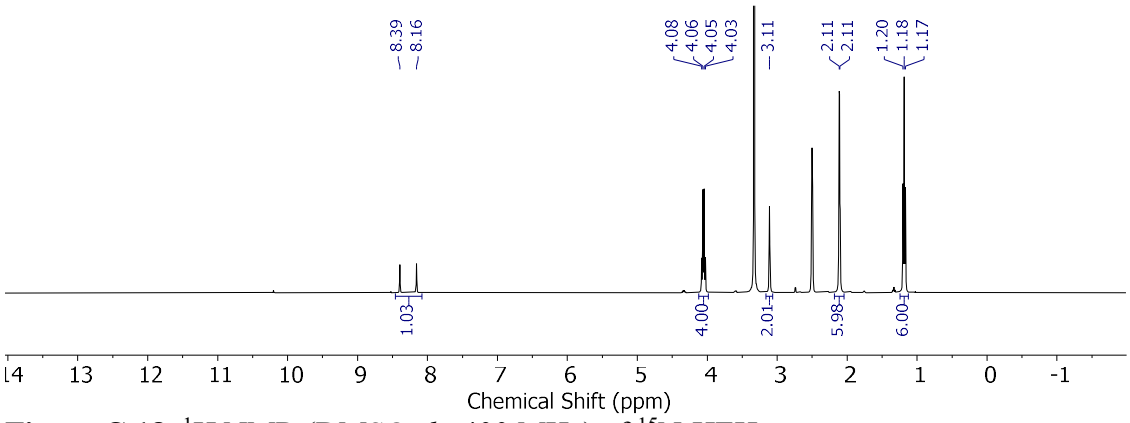

Figure C.18. ^{1}H NMR (DMSO-d_6, 400 MHz) of ^{15}N-HEH$_2$.

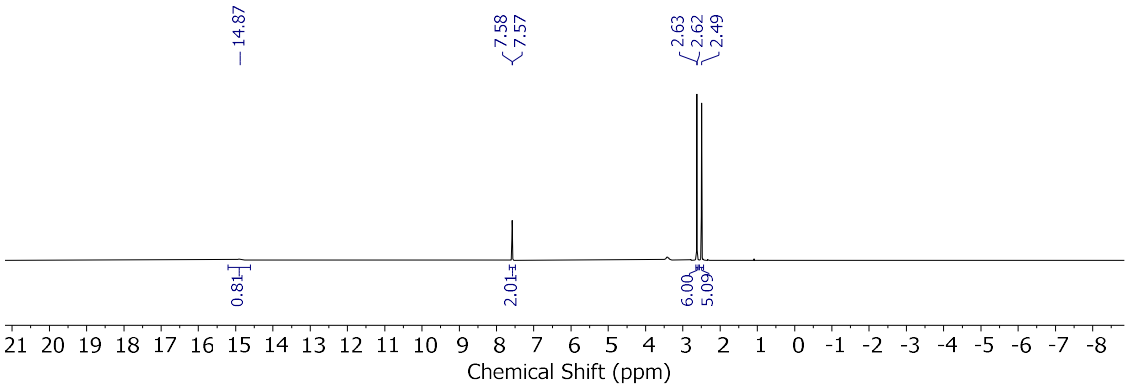

Figure C.19. ^{1}H NMR (DMSO-d_6, 400 MHz) of ^{15}N-labelled [ColH]OTf.

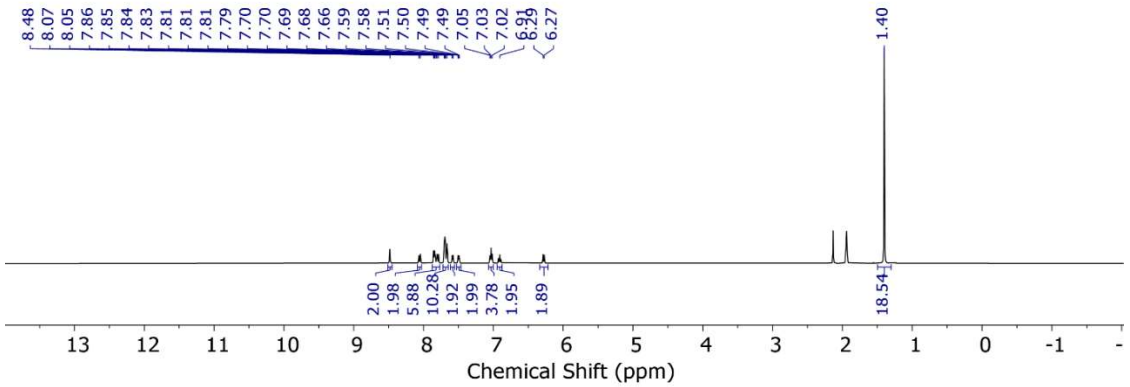

Figure C.20 ^{1}H NMR (MeCN-d_3, 400 MHz) of [Ir]BAr$^{F}_4$.

C.10 References for Appendix

1. Norcross, B. E.; Clement, G.; Weinstein, M.; *J. Chem. Educ.* **1969**. 46, 694.
2. Arashiba, K.; Eizawa, A.; Tanaka, H.; Nakajima, K.; Yoshizawa, K.; Nishibayashi, Y. *Bull. Chem. Soc. Jpn*. **2017**. 90, 1111–1118.
3. Anderson, J. S.; Moret, M. E.; Peters, J. C. *J. Am. Chem. Soc*. **2013**. 135, 534–537.
4. Shen, G.-B.; Fu, Y.-H.; Zhu, X.-Q. *J. Org. Chem*. **2020**. 85, 12535–12543.
5. Del Castillo, T. J.; Thompson, N. B.; Peters, J. C. *J. Am. Chem. Soc.* **2016**. 138, 5341–5350.
6. N. S. Golubev, S. N. Smirnov, P. Schah-Mohammedi, I. G. Shenderovich, G. S. Denisov, V. A. Gindin, H. H. Limbach, *Russ. J. Gen. Chem.* **1997**. 67, 1082–1087.
7. Matesic, L.; Locke, J. M.; Vine, K. L.; Ranson, M.; Bremner, J. B.; Skropeta D. *Tetrahedron* **2012**. 68, 6810–6819.
8. Brišar, R.; Unglaube, F.; Hollmann, D.; Jiao, H.; Mejía, E. *J. Org. Chem.* **2018**. 83, 13481–13490.
9. Elrod, L. T.; Kim, E. *Inorg. Chem*. **2018**. 57, 2594–2602.
10. Fulmer, G. R.; Miller, A. J. M.; Sherden, N. H.; Gottlieb, H. E.; Nudelman, A.; Stoltz, B. M.; Bercaw, J. E.; Goldberg, K. I. *Organometallics*. **2010**. 29, 2176–2179.
11. Weatherburn, M. W. *Anal. Chem.* **1967**. 39, 971–974.
12. Watt, G. W.; Chrisp, J. D. *Anal. Chem.* **1952**. 24, 2006–2008.
13. Xu, S.; Ashley, D. C.; Kwon, H.-Y.; Ware, G. R.; Chen, C.-H.; Losovyj, Y.; Gao, X.; Jakubikova, E.; Smith, J. M. *Chem. Sci*. **2018**. 9, 4950–4958.
14. Lindley, B. M.; Appel, A. M.; Krogh-Jespersen, K.; Mayer, J. M.; Miller, A. J. M. *ACS Energy Lett*. **2016**. 1, 698–704.
15. Gibanel, F.; López, M. C.; Royo, F. M.; Santafé, J.; Urieta, J. S. *J. Solution Chem*. **1993**. 22, 211–217.

16. Agarwal, R. G.; Coste, S. C.; Groff, B. D.; Heuer, A. M.; Noh, H.; Parada, G. A.; Wise, C. F.; Nichols, E. M.; Warren, J. J. ; Mayer, J. M. *Chem. Rev*. **2022**. 122, 1–49.
17. Jung, J.; Kim, J.; Park, G.; You, Y.; Cho, E. J. *Adv. Synth. Catal*. **2016**. 358, 74–80.
18. Ilic, S.; Pandey Kadel, U.; Basdogan, Y.; Keith, J. A.; Glusac, K. D. *J. Am. Chem. Soc*. **2018**. 140, 4569–4579.
19. Ilic, S.; Pandey Kadel, U.; Basdogan, Y.; Keith, J. A.; Glusac, K. D. *J. Am. Chem. Soc*. **2018**. 140, 4569–4579.
20. Tshepelevitsh, S.; Kütt, A.; Lõkov, M.; Kaljurand, I.; Saame, J.; Heering, A.; Plieger, P. G.; Vianello, R.; Leito, I. *Eur. J. Org. Chem*. **2019**. 2019, 6735–6748.
21. Slinker, J. D.; Gorodetsky, A. A.; Lowry, M. S.; Wang, J.; Parker, S.; Rohl, R.; Bernhard, S.; Malliaras, G. G. *J. Am. Chem. Soc*. **2004**. 126, 2763–2767.
22. Capacci, A. G.; Malinowski, J. T.; McAlpine, N. J.; Kuhne, J.; MacMillan, D. W. C. *Nat. Chem.* **2017**. 9, 1073–1077.
23. Koike, T.; Akita, M. *Inorg. Chem. Front*. **2014**. 1, 562–576.